

Loss of preloading in DTI assemblies and criteria for using DTIs in slip-resistant connections

Deliverable report D3.3

WP 3 – Task 3.3

Prof. Dr.-Ing. habil. Natalie Stranghöner

natalie.stranghoener@uni-due.de

Nariman Afzali M.Sc.

nariman.afzali@uni-due.de

Christoph Abraham, B.Sc.

christoph.abraham@uni-due.de

Part of the RFCS Research Project

“SIROCO”

Execution and reliability of slip-resistant connections for steel structures using CS and SS

RFCS Project No.: RFSR-CT-2014-00024

Project No. 410410007-20003

Report No.: 2018-04

Table of contents	Page
1 Scope of investigation	5
2 Design and execution according to the Eurocode	5
3 Experimental investigations	6
3.1 Compression tests	7
3.2 Tightening tests	9
3.2.1 General and normative references	9
3.2.2 Test equipment and test setup	9
3.2.3 Test programme and evaluation criteria	12
3.2.4 Test results	13
3.3 Relaxation tests	16
3.3.1 Test specification	16
3.3.2 Test results	21
4 Conclusions	33
5 References	34
6 Annex A: Rate of loss of preload	35

1 Scope of investigation

EN 1090-2 [1] provides several tightening methods for preloading of bolting assemblies. The Direct Tension Indicator (DTI) method specified in EN 1090-2 is one of several methods for tightening preloaded bolting assemblies to ensure the proper preload level ($F_{p,C}$) of a bolt. Different types of DTI washers are available. The most common types of direct tension indicators are produced with hollow bumps/protrusions on one side of the washer which must bear against the unturned element.

These protrusions are plastically flattened by preloading the DTI, which can be installed either under the bolt head or the nut of a bolting assembly. The preloading force is applied by tightening the bolting assembly either by rotation of the nut or bolt. The properties of the geometry and material of the DTIs are adjusted in such a way that the residual gaps between the flattened protrusions are a measure of the preloading force. The use of the feeler gauges with predetermined thicknesses shall allow the indication whether the actual preloading force is above the minimum required preloading force $F_{p,C}$ or not. Because a uniform flattening is not achievable in practice, the number of feeler gauge entries into gaps respectively the number of their refusals at gap positions is the relevant inspection result to determine that $F_{p,C}$ has been achieved. To avoid any indentation of the protrusions into their contact surface instead of flattening, a sufficiently high hardness must be provided for the contact surface. Thus, nut and bolt face washers should be used.

The DTI washers can only indicate the minimum required preload level. With this method it is not possible to measure the amount of over tensioning, if over-tightening occurs. For this reason, it is not allowed to tighten the bolting assemblies by closing all gaps of the DTIs to prevent over tensioning of the bolts.

Since the protrusions on the DTIs have plastic deformation, they will not return to their original shape in case of relaxation. Hence, it is not possible to monitor the amount of bolt relaxation. Therefore, a comprehensive investigation on the loss of preload/relaxation behaviour of DTI assemblies was performed in frame of the European RFCS-research project "Execution and reliability of slip resistant connections for steel structures using CS and SS" SIROCO.

In order to investigate whether DTIs are applicable in slip-resistant connections, the potential of loss of preloading of the bolting assemblies due to the plastically deformed protrusions shall be investigated, because a significant loss of preloading over the life time has to be avoided in slip-resistant connections. This research will be carried out by means of relaxation tests on bolting assemblies in which the preload is achieved using tightening under consideration of DTIs.

2 Design and execution according to the Eurocode

The bolt can be tightened by rotating either the nut or the bolt. As the bolt is tightened these bumps are flattened and reduce the gap. The gap developed by the bumps can be measured with a feeler gauge, see Figure 1. When the gap reaches the specified size and the feeler gauge will no longer fit in the gap, the bolt has reached the appropriate pretension level.



Figure 1 Use of a feeler gauge to check the gap

According to EN 1090-2 it is necessary to position the DTI properly. Figure 2 shows different assembly configurations to position the DTIs. By knowing the position of the DTI with respect to the rotated component, the thickness of the feeler gauge can be selected. According to EN 14399-9 [2], the feeler gauge shall be used as a 'no go' inspection tool.

When the bolt and nut are tightened, as shown in Figure 2, by preloading the bolt the protrusions partially deform and reduce the gap. When the gap is closed to the specified dimension (0.40 mm for configuration (a) and 0.25 mm for configuration (b), see Table 1), it can be considered as feeler gauge refusal. When the number of feeler gauge refusals n_{refusal} at the gaps is more than half the number of protrusions, the bolt has reached the proper preload level. Otherwise the tightening procedure has to be continued and the $F_{p,C}$ has not been achieved yet. The flattening of the protrusions does not remain constant during the preloading process, for this reason closing of the gaps will not happen at the same time.

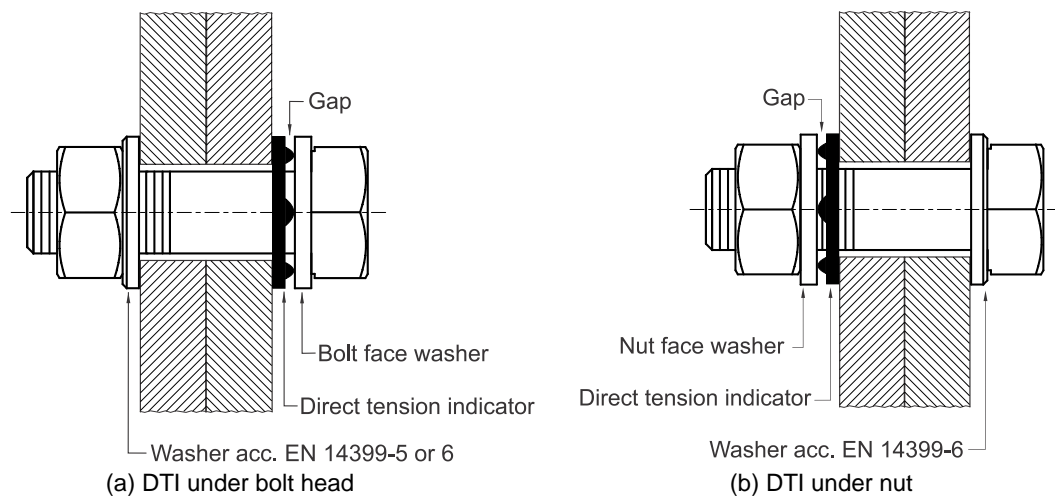


Figure 2 Assembly configurations according to EN 14399-9

Table 1 Proper thickness of the feeler gauge

Assembly configurations	Thickness of feeler gauge
When DTI is faced non-rotated component	0.40 mm
When DTI is faced rotated component	0.25 mm

3 Experimental investigations

The experimental investigations consisted of three different steps: in the first step, compression tests were performed to verify the mechanical performance of DTIs individually. In the second step, tightening and tensile tests were performed with a

combination of DTIs and HV bolting assemblies (according to EN 14399-4 [3]) to verify the suitability of using the DTI system. Finally, the relaxation tests were conducted on preloaded bolted connections using DTIs to investigate the potential of preload losses.

3.1 Compression tests

The compression tests were carried out at the Institute for Metal and Lightweight Structures of the University of Duisburg-Essen. A universal testing machine with a capacity of ± 200 kN was used. The specific test setup was arranged between the existing pressure plates, see Figure 3.



Figure 3 Test setup for compression test according to EN 14399-9

The compression tests were performed in two steps and the local displacement was measured continually by a displacement transducer (LVDT). In the first step, the DTI was placed on the support block with the protrusions facing down. In this position, the DTI was placed into a circular groove and there was no contact between the protrusions and the support block, see Figure 4(a).

According to the type and size of the DTI, a compression load up to a maximum of $F_{p,C}$ was applied. Further displacement measurement represented the height of the protrusions/gaps (h_{gap}). After unloading, the support block had to be turned so that face with the groove was facing down and the DTI also had to be inverted to the protrusions facing up, see Figure 4(b).

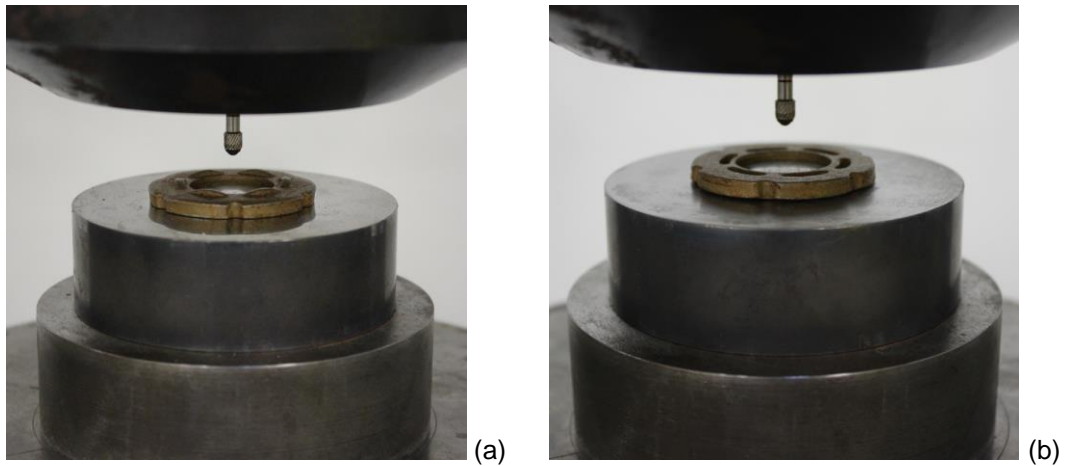


Figure 4 First and second steps during compression test according to EN 14399-9

Afterwards, the compression load was applied one more time until a LVDT reading of 0.4 mm was reached. The speed of the tests had to be adjusted in such a way that the 0.40 mm gap closed in 30 seconds. The corresponding compression load was recorded continually and the value had to be within $1.0 F_{p,c}$ and $1.2 F_{p,c}$ in order to pass the test successfully.

In total, six compression tests (three M16 and three M20) were performed to verify the mechanical performance. Figure 5 shows the gap - compression load diagram for each DTI individually. As it can be seen all DTIs fulfilled the requirements for the compression test, see Figure 5.

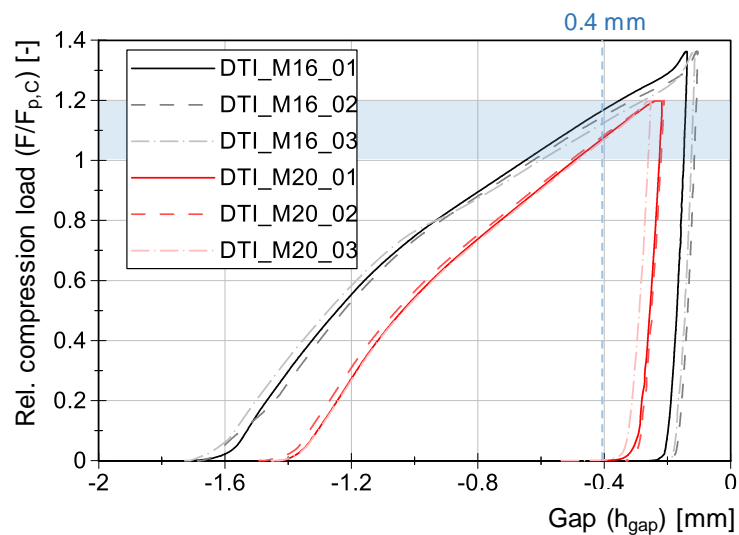


Figure 5 Gap - compression load diagram for each DTI

At the end, in order to find the maximum loading F_{max} , the compression load was increased to close all gaps. When all gaps were closed, the compression load was recorded as the maximum loading, see Table 2.

Table 2 Results of compression tests

Test ID	Test duration	Load at 0.4 mm	Testing rate	Maximum load	Relative load at 0.4 mm
	t [s]	$F_{0.4}$ [kN]	v_F [kN/s]	F_{max} [kN]	$F_{0.4} / F_{p,C}$ [-]
DTI – M16 – H10					
DTI-M16-01	30	128.6	4	150	1.17
DTI-M16-02	30	126.3	4	150	1.15
DTI-M16-03	30	124.0	4	150	1.13
DTI – M20 – H10					
DTI-M20-01	29	185.3	6	206	1.08
DTI-M20-02	29	186.7	6	206	1.09
DTI-M20-03	29	184.1	6	206	1.07

3.2 Tightening tests

3.2.1 General and normative references

In addition to the compression tests on the individual Direct Tension Indicators (DTIs), the suitability of the DTIs must be tested for use in combination with the intended bolting assembly of bolt, nut (acc. EN 14399-4 [3] for System HV) and washer (acc. EN 14399-6 [4] and EN 14399-9 [2]). In EN 14399-9, the „Suitability test for preloading with direct tension indicator in an assembly” is defined in subchapter 5.3.2.1 as well as the “Suitability test for establishing bolt force” in subchapter 5.3.2.2.

According to EN 1090-2, bolting assemblies for use with DTIs have to fulfill the requirements of k-classes K0, K1 or K2. Due to the influence of the lubrication or friction on the suitability, the bolting assemblies are usually lubricated by the bolt manufacturer. For this reason, the bolting assemblies were not lubricated additionally for tightening tests and relaxation tests to guarantee homogeneous testing conditions in accordance with EN 14399-9, see [5].

3.2.2 Test equipment and test setup

The suitability tests for preloading with DTIs were carried out with the tightening torque testing machine (maximum torque: 15000 Nm and maximum bolt force: 1800 kN) at the Institute for Metal and Lightweight Structures of the University of Duisburg-Essen, see Figure 6. The torque and rotation were automatically generated by an electric gear motor. The tightening speed is set manually via an adjusting gear before starting the tightening test and was constant for all tests 2.0 rpm to ensure accurate measurements especially regarding the angle of rotation and to avoid overtightening. The tightening torque testing machine is equipped with sensors for recording measurements from the company Schatz GmbH, Remscheid, Germany.

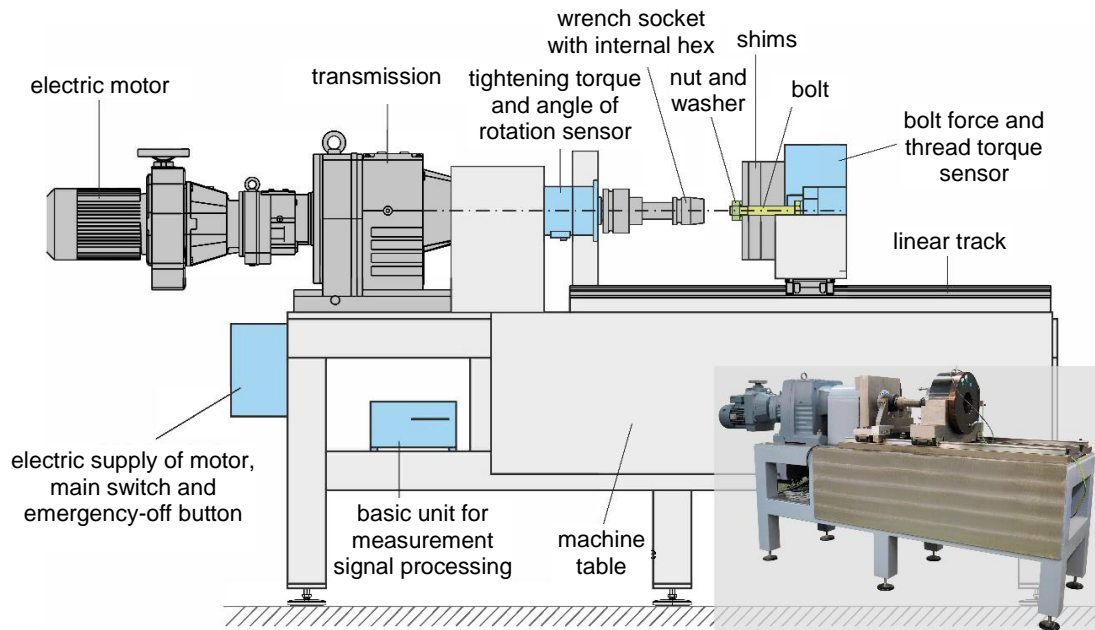


Figure 6 Tightening torque testing machine of Institute for Metal and Lightweight Structures of University of Duisburg-Essen

The test procedure is based on the requirements according to EN 14399-2 [6] and incorporates requirements applicable to assemblies which include DTIs. In addition, the requirements regarding sufficient ductility of carbon steel HV bolting assemblies are specified in EN 14399-4. From these four criteria, only the requirements (2) and (4), see following equations (2) and (4), have to be fulfilled on $F_{p,C}$ -level in the suitability test for preloading acc. to EN 14399-2/4. Criterion (4) is modified by EN 14399-9. A schematic overview on a typical bolt force-angle of rotation curve (left) and bolt force-tightening torque curve (right) according to EN 14399-2 are presented in Figure 7.

$$\square F_{p,C} = 0.7 \cdot f_{ub} \cdot A_s \quad (1)$$

$F_{p,C}$ specified preloading level (see also EN 1090-2)

f_{ub} nominal tensile strength ($R_{m,nom}$) of the bolt

A_s nominal stress area of the bolt (see EN ISO 898-1)

$$\square F_{bi,max} \geq 0.9 \cdot f_{ub} \cdot A_s \quad (2)$$

$F_{bi,max}$ individual value of the maximum bolt force reached during the test

f_{ub} nominal tensile strength ($R_{m,nom}$) of the bolt

A_s nominal stress area of the bolt

$$\square \Delta\Theta_{1i} \geq \Delta\Theta_{1,min} = 90^\circ / 120^\circ / 150^\circ \text{ (depending on the clamp length)} \quad (3)$$

$\Delta\Theta_{1i}$ individual angle difference of the nut from the first time the preload $F_{p,C}$ is exceeded to the individual value of the maximum bolt force $F_{bi,max}$

$$\square \Delta\Theta_{2i} \geq \Delta\Theta_{2,min} = 210^\circ / 240^\circ / 270^\circ \text{ (depending on the clamp length)} \quad (4)$$

$\Delta\Theta_{2i}$ individual angle difference of the nut from the first time the preload $F_{p,C}$ is exceeded to the angle when bolt force drops below $F_{p,C}$ again

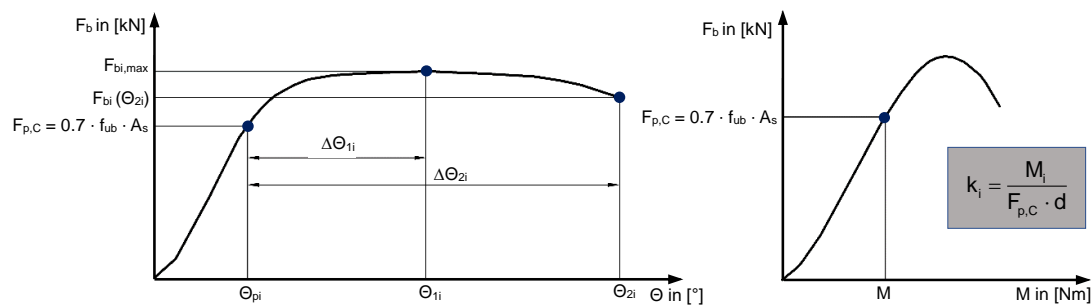


Figure 7 Schematic bolt force-angle of rotation curve (left) and bolt force-tightening torque curve (right) according to EN 14399-2

Suitability tests for DTI under the bolt head and under the nut require a special test setup to check continuously the gap from all sides between the direct tension indicator protrusions during tightening to previously defined load steps. The test setup for testing the DTI under the nut for bolt dimensions M16x65 and M20x115 is presented in Figure 8. The test setup for testing the DTI under the bolt head requires the inverse alignment of the preload/thread torque sensor. Furthermore, it is necessary to fix the bolt head with an auxiliary construction to prevent twisting of the bolt head during the tightening procedure. The test setup for bolt dimension M20x115 HV 10.9 is presented in Figure 9, whereas for bolt dimension M16x65 HV 10.9 the suitability test for the use of DTIs under the bolt head was not possible due to limitations of the test setup and the chosen clamping lengths.

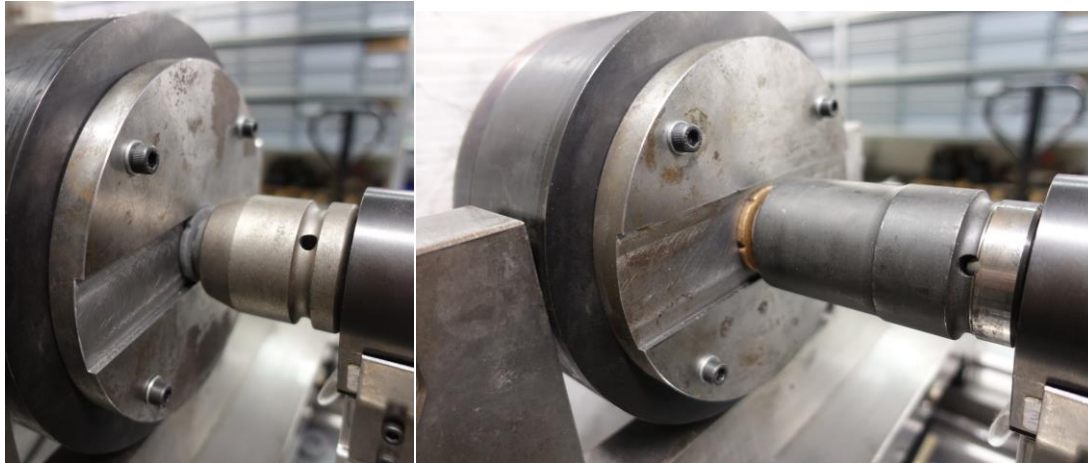


Figure 8 Test setup for M16x65 HV 10.9 bolting assemblies with DTI placed under the nut (left) and test setup for M20x115 HV 10.9 bolting assemblies with DTI placed under the nut (right)

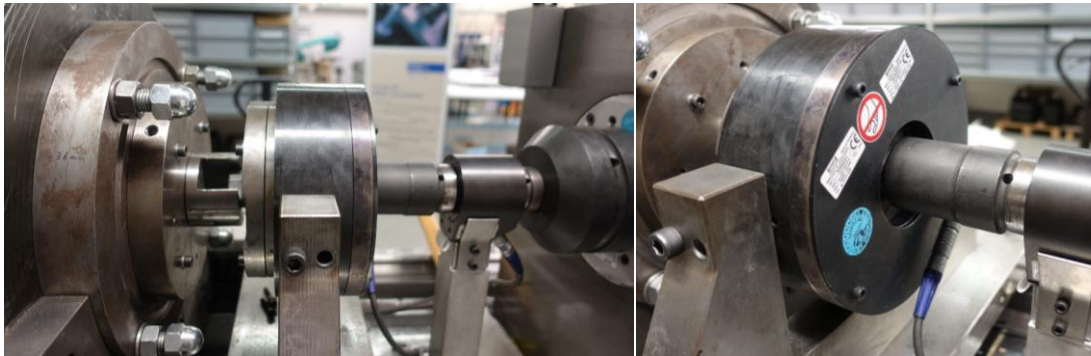


Figure 9 Test setup for M20x115 HV 10.9 bolting assemblies with DTI placed under the bolt head

3.2.3 Test programme and evaluation criteria

The suitability tests were carried out on the basis of EN 14399-2/4 and EN 14399-9. The investigated bolting assemblies exist of bolts and nuts according to EN 14399-4 System HV M20x115 and M16x65, property class 10.9 with plain chamfered washers according to EN 14399-6 and nut face washers as well as bolt face washers according to EN 14399-9. The bolting assemblies before testing are exemplarily shown in Figure 10.



Figure 10 M16x65 HV 10.9 and M20x115 HV 10.9 bolting assemblies before testing including bolt face and nut face washers

The test matrix of the suitability tests is shown in Table 3 and gives an overview about the used components, the number of tests and the clamping length/bolt diameter ratio. In total, seven bolting assemblies were tested to evaluate the suitability for preloading of direct tension indicators under the bolt head and under the nut.

Table 3 Test matrix for suitability tests for preloading with direct tension indicators

Test specifications				Components		
Test ID	Number of tests	$\Sigma t/d$ ¹⁾ [-]	Position of the DTI ²⁾	Bolt/Nut	Washer under the bolt head	Washer under the nut
M16-N	3	2.81	under the nut	M16x65 HV 10.9 acc. EN 14399-4	-	Nut face washer acc. EN 14399-9
M20-N	2	4.50	under the nut	M20x115 HV 10.9 acc. EN 14399-4	-	Nut face washer acc. EN 14399-9
M20-B	2	4.50	under the bolt head	M20x115 HV 10.9 acc. EN 14399-4	Bolt face washer acc. EN 14399-9	Plain chamfered washer acc. EN 14399-6

¹⁾ clamp length-bolt diameter ratio | ²⁾ Assembly configuration acc. Figure 7 of EN 14399-9.

The evaluation of the suitability for preloading of direct tension indicators under the bolt head and under the nut is referred to subchapter 5.3.2.1 and subchapter 5.3.2.2 of EN 14399-9. Initial type tests shall be carried out separately for direct tension indicators under the bolt head and under the nut. The initial type test shall be used to demonstrate that $\Delta\Theta_2$ - measured with assemblies including a direct tension indicator - exceeds $\Delta\Theta_{2,min}$ (which depends on the clamping length) by at least 10 %. In addition, the criterion of individual maximum bolt force $F_{bi,max} \geq 0.9 \cdot f_{ub} \cdot A_s$ must be fulfilled.

3.2.4 Test results

3.2.4.1 Bolt dimension M16 – DTI nut side

The test results of M16x55 HV 10.9 bolting assemblies with direct tension indicators under the nut are presented in Table 4 and Table 5. It can be seen that the suitability tests failed for every tested bolting assembly. The tested assemblies exceed $1.1 \cdot \Delta\Theta_{2,min}$, but the criterion of individual maximum bolt force $F_{bi,max} \geq 0.9 \cdot f_{ub} \cdot A_s$ was slightly not achieved by 1.4 % to 7.6 %.

Table 4 Feeler gauge refusals – Suitability test for preloading with DTI according to EN 14399-9 (5.3.2) for bolt dimension M16x65 and DTI placed under the nut

Test ID	Sample	Bolt force F_b [kN]							Status		
		94	102	110	117	124	132				
		Ratio $F_b / F_{b,C}$		1,00		1,06		1,13		1,20	
		Thickness of feeler gauge [mm]		Number of feeler gauge refusals**							
M16-HN-1	HV + DTI according to EN 14399-9, Figure 7b	0,4	0	3	4	-	-	-	-	-	-
		0,25*	0	0	2	4	-	-	-	-	passed
M16-HN-2	HV + DTI according to EN 14399-9, Figure 7b	0,4	0	0	0	4	4	4	4	4	-
		0,25*	0	0	0	0	3	4	4	4	passed
M16-HN-3	HV + DTI according to EN 14399-9, Figure 7b	0,4	0	0	1	2	4	4	4	4	-
		0,25*	0	0	0	0	2	4	4	4	passed

*normative for selected configuration

**minimum number of feeler gauge refusals = 3

Table 5 Angle of rotation and maximum individual bolt force – Suitability test for preloading with DTI according to EN 14399-9 (5.3.2) for bolt dimension M16x65 and DTI placed under the nut

Test ID	$F_{bi,max}$ [kN]	Angle of rotation			Status
		$\Delta\theta_{2i,min}$	$1,1 \Delta\theta_{2i,min}$	$\Delta\theta_{2i}$	
M16-HN-1	131	210	231	313	failed
M16-HN-2	138	210	231	317	failed
M16-HN-3	139	210	231	343	failed

Exemplarily, the tightening curves of test specimen M16-HN-2 are presented in Figure 11. The specified preload level $F_{p,C} = 0.7 \cdot f_{ub} \cdot A_s = 110$ kN, the required angle of nut rotation $1.1 \cdot \Delta\theta_{2,min} = 231^\circ$ and the criterion of maximum individual bolt force $F_{bi,max} \geq 0.9 \cdot f_{ub} \cdot A_s = 141$ kN are also presented.

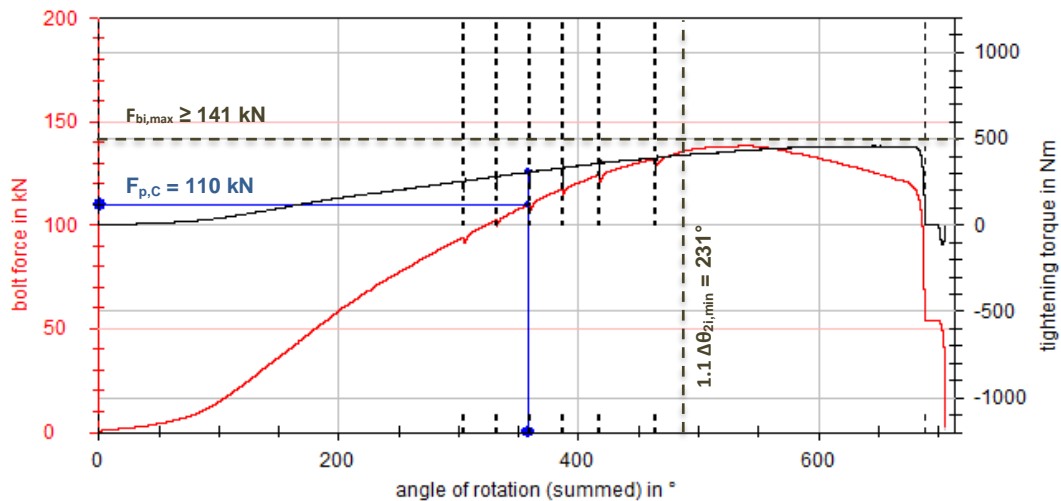


Figure 11 Tightening curves of test specimen M16-HN-2

3.2.4.2 Bolt dimension M20 – DTI nut side

The test results of M20x115 HV 10.9 bolting assemblies with direct tension indicators under the nut are presented in Table 6 and Table 7. It can be seen that the suitability tests were passed for every tested bolting assembly. The tested assemblies exceed $1.1 \cdot \Delta\theta_{2,min}$, and the criterion of individual maximum bolt force $F_{bi,max} \geq 0.9 \cdot f_{ub} \cdot A_s$ is achieved as well.

Table 6 Feeler gauge refusals – Suitability test for preloading with DTI according to EN 14399-9 (5.3.2) for bolt dimension M20 and DTI placed under the nut

Test ID	Sample	Bolt force F_b [kN]		148	160	172	183	195	206	Status
		Ratio $F_b / F_{p,C}$		0,86	0,93	1,00	1,06	1,13	1,20	
		Thickness of feeler gauge [mm]		Number of feeler gauge refusals**						
M20-HN-1	HV + DTI according to EN 14399-9, Figure 7b	0,4		2	4	4	5	5	6	-
		0,25*		2	2	2	3	4	6	passed
M20-HN-2	HV + DTI according to EN 14399-9, Figure 7b	0,4		2	4	6	6	6	-	-
		0,25*		0	1	2	4	6	-	passed

*normative for selected configuration

**minimum number of feeler gauge refusals = 4

Table 7 Angle of rotation and maximum individual bolt force – Suitability test for preloading with DTI according to EN 14399-9 (5.3.2) for bolt dimension M20 and DTI placed under the nut

Test ID	F _{bi,max} [kN]	Angle of rotation			Status
		Δθ _{2i,min}	1,1 Δθ _{2i,min}	Δθ _{2i}	
M20-HN-1	254	210	231	302	passed
M20-HN-2	253	210	231	312	passed

Again, the tightening curves of test specimen M20-HN-1 are exemplarily presented in Figure 12. The specified preload level $F_{p,C} = 0.7 \cdot f_{ub} \cdot A_s = 172 \text{ kN}$, the required angle of nut rotation $1.1 \cdot \Delta\theta_{2,min} = 231^\circ$ and the criterion of maximum individual bolt force $F_{bi,max} \geq 0.9 \cdot f_{ub} \cdot A_s = 221 \text{ kN}$ are also given.

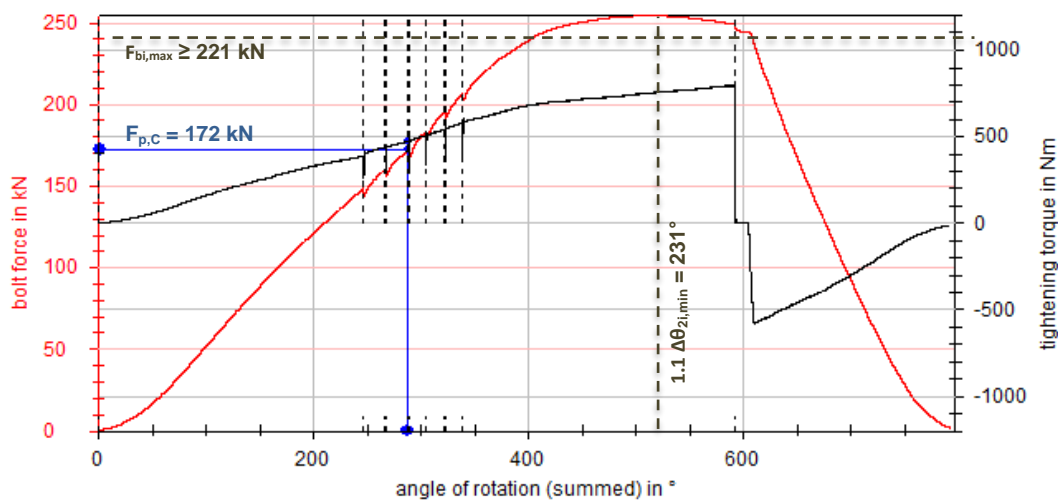


Figure 12 Tightening curves of test specimen M20-HN-1

3.2.4.3 Bolt dimension M20 – DTI bolt head side

The test results of M20x115 HV 10.9 bolting assemblies with DTIs under the bolt head are presented in Table 8 and Table 9. It can be seen that the suitability tests failed for every tested bolting assembly. Nevertheless, the tested assemblies exceeded $1.1 \cdot \Delta\theta_{2,min}$, and the criterion of individual maximum bolt force $F_{bi,max} \geq 0.9 \cdot f_{ub} \cdot A_s$ was also achieved.

Table 8 Feeler gauge refusals – Suitability test for preloading with DTI according to EN 14399-9 (5.3.2) for bolt dimension M20 and DTI placed under the bolt head

Test ID	Sample	Bolt force F _b [kN]		148	160	172	183	195	206	Status
		Ratio F _b / F _{p,C}		0,86	0,93	1,00	1,06	1,13	1,20	
		Thickness of feeler gauge [mm]	Number of feeler gauge refusals**							
M20-HB-1	HV + DTI according to EN 14399-9, Figure 7b	0,4*	5	6	6	-	-	-	-	failed
		0,25	1	4	6	-	-	-	-	-
M20-HB-2	HV + DTI according to EN 14399-9, Figure 7b	0,4*	3	4	5	6	6	6	6	failed
		0,25	2	3	4	4	5	6	6	-

*normative for selected configuration

**minimum number of feeler gauge refusals = 4

Table 9 Angle of rotation and maximum individual bolt force – Suitability test for preloading with DTI according to EN 14399-9 (5.3.2) for bolt dimension M20 and DTI placed under the bolt head

Test ID	$F_{bi,max}$ [kN]	Angle of rotation			Status
		$\Delta\theta_{2i,min}$	$1,1 \Delta\theta_{2i,min}$	$\Delta\theta_{2i}$	
M20-HB-1	240	210	231	298	passed
M20-HB-2	234	210	231	299	passed

The tightening curves of test specimen M20-HB-1 are exemplarily presented in Figure 13. The specified preload level $F_{p,C} = 0.7 \cdot f_{ub} \cdot A_s = 172$ kN, the required angle of nut rotation $1.1 \cdot \Delta\theta_{2i,min} = 231^\circ$ and the criterion of the maximum individual bolt force $F_{bi,max} \geq 0.9 \cdot f_{ub} \cdot A_s = 221$ kN are given as well.

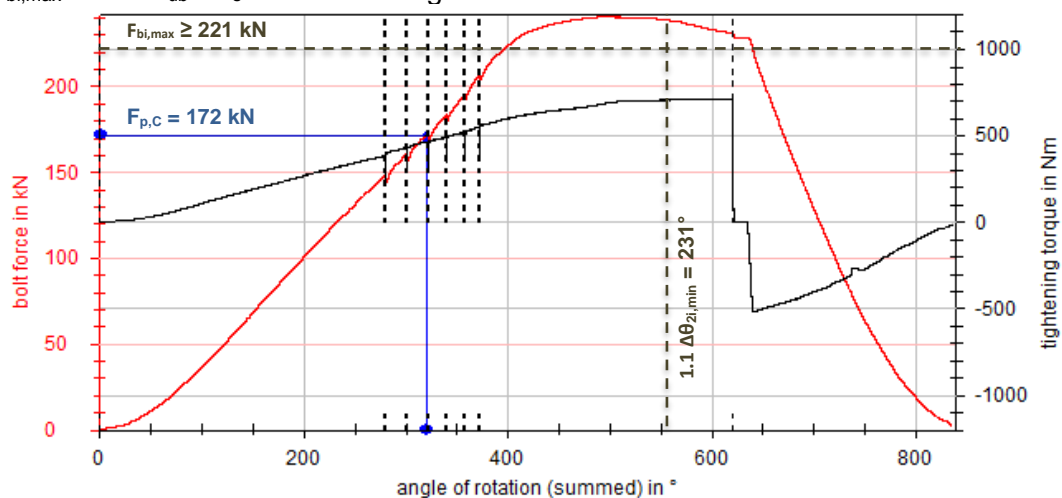


Figure 13 Tightening curves of test specimen M20-HB-1

3.3 Relaxation tests

3.3.1 Test specification

Within the project, carbon steel components and M20 and M16 HV-bolting assemblies with property class 10.9 according to EN 14399-4 [3] were used for experimental testing of the loss of preload of DTIs bolting assemblies. Two different configurations were selected to investigate the influence of positioning of DTIs on the achieved preload level and preload losses. In addition, for each bolt dimension different clamping lengths were considered in order to investigate the influence of the clamping length on the relaxation behaviour of bolted connections. The clamping lengths were selected in such a way that the calculated clamping length ratios were the same for different bolt dimensions with or without DTIs. The clamping length ratios can be categorized in three different groups: series with clamping length ratio of about 1.5, 2.5 and 4.5.

To measure the preload in bolting assemblies, all bolts were instrumented with implanted strain gauges at the Institute for Metal and Lightweight Structures of the University of Duisburg-Essen (UDE). All HV bolts of size M20 and M16 with property class 10.9 and three different lengths were manufactured by drilling a centric hole of 2 mm diameter along the bolt shank. After drilling, the holes were cleaned and degreased. Two components of an adhesive were mixed and injected into the hole by using a syringe.

BTM-6C and BTM-1C (produced by Tokyo Sokki Kenkyujo Co., Ltd.) strain gauges were used for instrumentation of the bolts, see Figure 14.

Table 10 Test matrix for the relaxation tests of bolted assemblies made of carbon and stainless steel

Ser. ID	Type of specimen	Number of tests	$\Sigma t/d$ ¹⁾ [-]	Bolt		Clamped plates		Surface cond.	
				Dimension	P _c ²⁾ [-]	F _p ³⁾ [kN]	Material type		Dims. [cm]
M20 10.9 bolts with DTI									
DTI01	8 bolt	First row	4	1.6	HV M20 x 55	10.9	F _{p,C}	S355	as received
		Sec. row	4						
	1 bolt	-	3						
DTI02	8 bolt	First row	4	2.6	HV M20 x 75	10.9	F _{p,C}	S355	as received
		Sec. row	4						
	1 bolt	-	2						
DTI03	8 bolt	First row	4	4.6	HV M20 x 115	10.9	F _{p,C}	S355	as received
		Sec. row	4						
	1 bolt	-	4						
M20 10.9 bolts without DTI									
DTI04	8 bolt	First row	3	1.4	HV M20 x 55	10.9	F _{p,C}	S355	as received
		Sec. row	3						
	1 bolt	-	2						
DTI05	8 bolt	First row	4	2.4	HV M20 x 75	10.9	F _{p,C}	S355	as received
		Sec. row	4						
	1 bolt	-	3						
DTI06	8 bolt	First row	4	4.4	HV M20 x 115	10.9	F _{p,C}	S355	as received
		Sec. row	-						
	1bolt	-	4						
M16 10.9 bolts with DTI									
DTI07	8 bolt	First row	4	1.7	HV M16 x 45	10.9	F _{p,C}	S355	as received
		Sec. row	3						
	1bolt	-	2						
DTI08	8 bolt	First row	4	2.7	HV M16 x 65	10.9	F _{p,C}	S355	as received
		Sec. row	4						
	1bolt	-	3						
DTI09	8 bolt	First row	-	4.7	HV M16 x 95	10.9	F _{p,C}	S355	as received
		Sec. row	-						
	1bolt	-	4						
M16 10.9 bolts without DTI									
DTI10	8 bolt	First row	3	1.5	HV M16 x 45	10.9	F _{p,C}	S355	as received
		Sec. row	3						
	1bolt	-	2						
DTI11	8 bolt	First row	4	2.5	HV M16 x 65	10.9	F _{p,C}	S355	as received
		Sec. row	4						
	1bolt	-	3						
DTI12	8 bolt	First row	4	4.5	HV M16 x 95	10.9	F _{p,C}	S355	as received
		Sec. row	4						
	1bolt	-	2						

¹⁾ clamping length ratio ($\Sigma t =$ clamping length and $d =$ bolt dimension) | ²⁾ property class | ³⁾ preload level |

* In the first row of the 8 bolts specimens, the DTIs were placed under the bolt heads and in the second row, the DTIs were placed under the nuts.

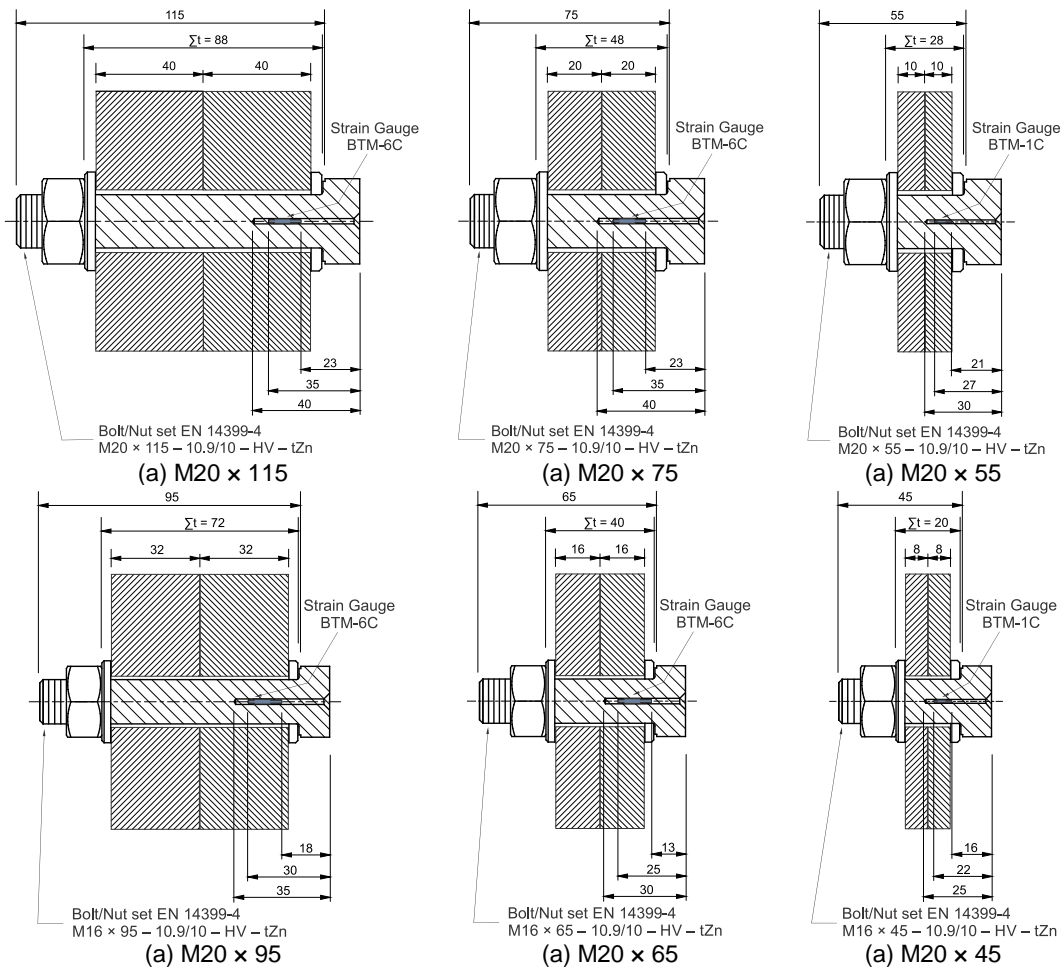


Figure 14 Instrumentation of bolts by implanted strain gauges

The strain gauge has to be inserted gently into the hole to a certain depth while holding the upper part of the lead. In the next step, the bolts are placed in a glass vacuum desiccator. For 15 min to 20 min, a vacuum has to be created to get a level of 1 Pa to 10 Pa. Thereafter, the bolts are placed in an electric furnace at 140°C for a period of 3 hours, see Figure 15. Hereby, the temperature has to be increased slowly to avoid the appearance of air bubbles or cracks in the adhesive. Afterwards, each instrumented bolt has to be calibrated under stepwise tensile loading. In the frame of SIROCO, this was carried out using a universal testing machine with a capacity of ± 200 kN, for more information see [7]. Those bolts, which showed a linear load-strain behaviour, were selected for application within the relaxation tests.

The test specimens were prepared by the Institute for Metal and Lightweight Structures (IML) of the University of Duisburg-Essen. All test series were conducted with S355 carbon steel plates according to EN 10025-2 [8] in the "as received" surface condition, see Figure 16.

For each bolt dimension, three different clamping lengths were selected, see Figure 14, and for each clamping length, the relaxation tests were performed with and without DTIs.

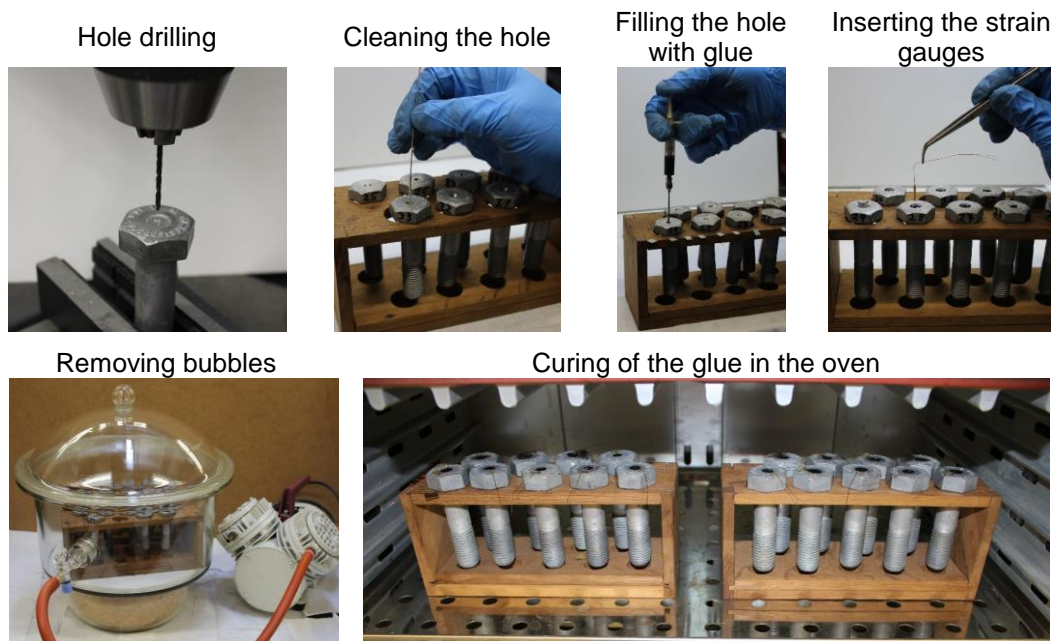
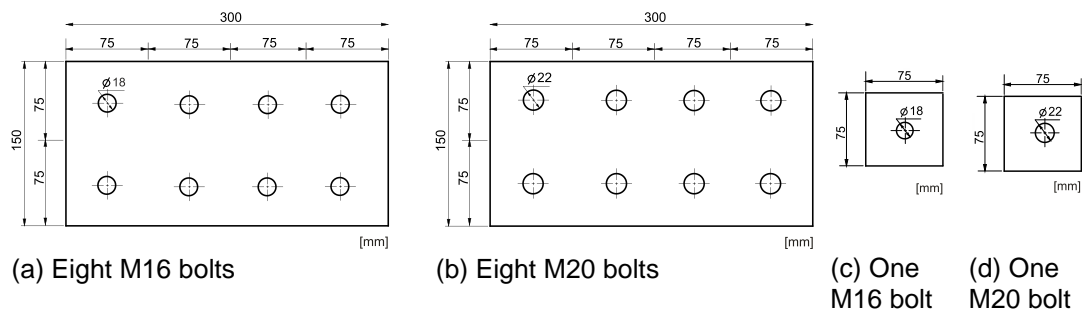


Figure 15 Production of the implanted strain gauges at UDE

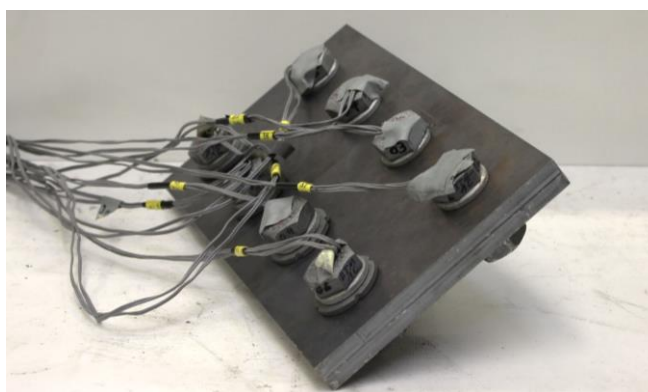


(a) Eight M16 bolts

(b) Eight M20 bolts

(c) One M16 bolt

(d) One M20 bolt



(e) Eight-bolt-specimen (150 mm x 150 mm plates)



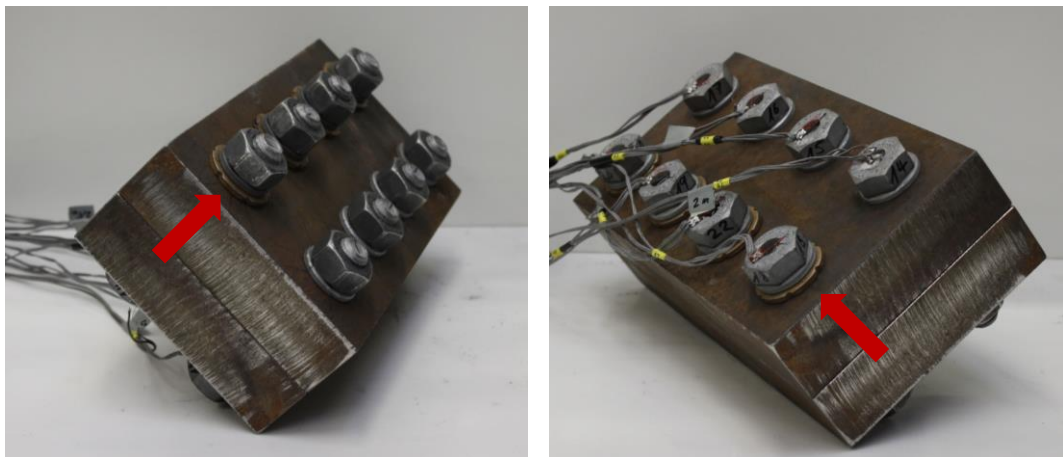
(f) One-bolt-specimen (75 mm x 75 mm plates)

Figure 16 Test specimen geometry for the relaxation tests of the bolted connections (test specimens for M16 and M20 bolts)

Two different assembly configurations according to EN 14399-9 (see Figure 2) were selected in order to investigate the influence of positioning of the DTIs on the

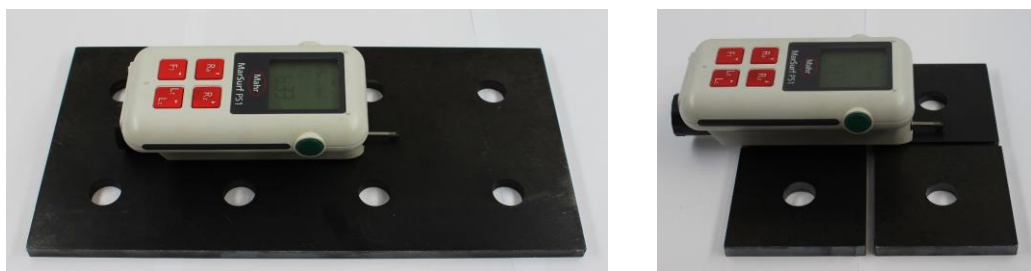
relaxation behaviour of the bolting assemblies. For the eight-bolt-specimens, the DTIs were placed under the bolt heads in the first row and under the nuts in the second row. For all one-bolt-specimens, the DTIs were placed under the nut, see Figure 16 and Figure 17. In both combinations, the preload was applied by turning the nut. With respect to the rotated component and the position of DTIs, the thickness of the feeler gauge was selected.

The surface roughness was measured for all surfaces by the Institute for Metal and Lightweight Structures of the University of Duisburg-Essen according to EN ISO 4287 [9] in the bolt hole areas, see Figure 18, using the MarSurf PS1 roughness measurement device from Mahr GmbH. The measured roughness Rz of the faying surfaces varied from 6 µm to 12 µm.

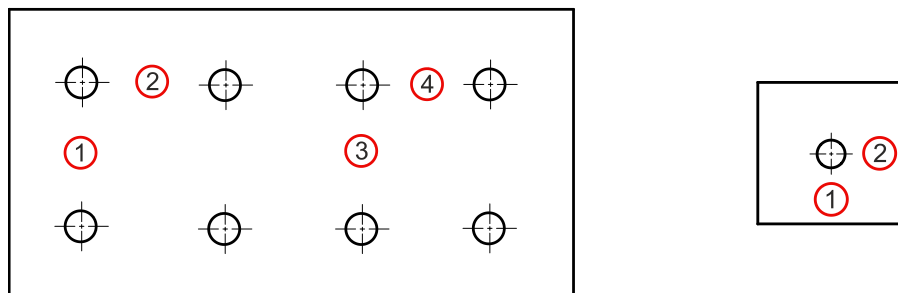


(a) In the first row, all DTIs are placed under the nut (b) In the second row, all DTIs are placed under the bolt head

Figure 17 Position of the DTIs in the eight-bolt-specimen



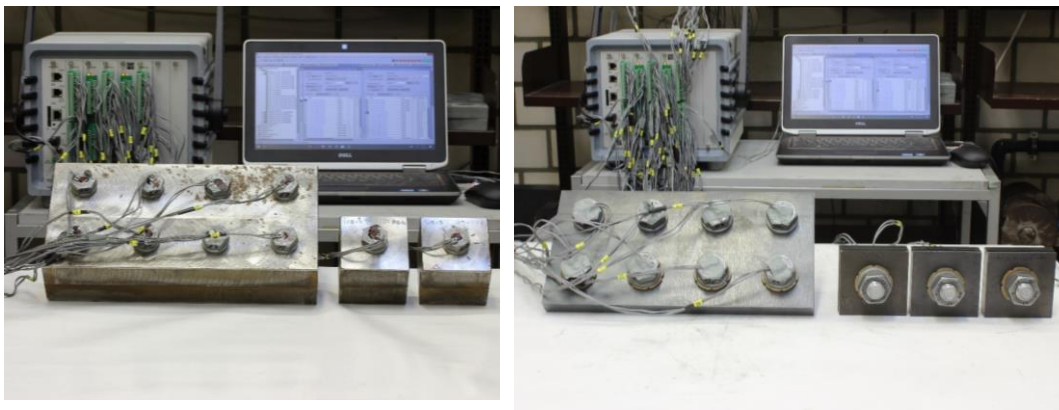
(a) Measurement of the surface roughness (MarSurf PS1 roughness measurement device from Mahr GmbH)



(b) Number and position of the measurement

Figure 18 Measuring of the surface roughness

In the series with DTIs, the preload was applied in different steps. The residual gaps between the flattened protrusions were measured in each step until the number of feeler gauge refusals n_{refusal} at the gaps was more than half the number of protrusions. For all other test series (without DTIs), the preload level of $F_{p,C} = 0.7 \cdot f_{ub} \cdot A_s$ according to EN 1090-2 [1] (with f_{ub} : nominal tensile strength of the bolt and A_s : tensile stress area of the bolt) was considered. Herewith, the preload level for M20 and M16 HV 10.9 bolts yielded to about 172 kN and 110 kN respectively. The preload was measured continuously during the tests for all test series, see Figure 19.



(a) Exemplary test setup for M16 bolted connection without DTIs

(b) Exemplary test setup for M20 bolted connection with DTIs

Figure 19 Test setup

3.3.2 Test results

The resulting preload losses of the bolting assemblies after testing were extrapolated to 50 years, see Table 11 and Table 12. In order to have a rational evaluation of the measurements, the first three seconds of the measurements were not taken into account. After tightening of the bolts, a considerable drop in the measured preload curve between the maximum peak and the first seconds after tightening can be observed. This instant drop is not entirely related to the relaxation behaviour of the bolting assemblies. However, this phenomenon is explained by turning back of the nut and elastic recovery of the bolt threads when the wrench is removed; it is the so-called overshoot effect. For this reason, this overshoot has to be extracted. By removing the first three seconds and by considering the linear behaviour of the loss of preload in a logarithmic scale, it is possible to derive the exact starting point of the relaxation test. Figure 20 to Figure 31 show the preload losses-log (time) diagrams for all different series M20 and M16 with and without DTIs with three different clamping length ratio categories.

As it can be seen in Table 11 and Table 12, the smaller clamping length leads to higher loss of preload in the preloaded bolting assemblies. This phenomenon can be confirmed for both bolt dimensions, with or without DTIs.

The results show that the highest loss of preload for M20 bolting assemblies with DTIs was observed by about 16 % which is higher in comparison to the loss of preload resulting for M16 bolting assemblies with DTIs with a similar clamping length ratio of about 10 %, see Figure 32. It can also be seen from Table 11 and Table 12 that the

amount of loss of preload for bolting assemblies without DTIs between the two different dimensions of bolts (M16 and M20) is comparable.

Table 11 Relaxation test results of M20 bolting assemblies with/without DTIs

Ser. ID	Type of specimen	No. of tests	$\Sigma t/d$ ¹⁾ [-]	Bolt			Clamped plates			
				Dimension	P _c ²⁾ [-]	F _p ³⁾ [kN]	Mater. type	measured after days - min / mean / max [%]	after 50 years (extrapolated) min / mean / max [%]	
M20 10.9 bolts with DTI										
DTI01	8 bolt	First row	4	1.6	HV M20 x 55	10.9	S355	0-4	20 – 9.3 / 10.1 / 11.4	14.3 / 15.9 / 17.4
		Sec. row	4					0-4	20 – 9.7 / 10.5 / 11.1	15.7 / 16.6 / 17.9
	1 bolt	-	3					1-3	35 – 9.3 / 10.1 / 10.8	13.8 / 14.9 / 15.9
DTI02	8 bolt	First row	4	2.6	HV M20 x 75	10.9	S355	4-4	45 – 9.0 / 9.8 / 10.4	12.5 / 13.4 / 14.2
		Sec. row	4					2-4	45 – 10.7 / 11.6 / 13.0	15.4 / 16.6 / 18.1
	1 bolt	-	2					1-2	45 – 10.0 / 10.2 / 10.3	14.0 / 14.3 / 14.6
DTI03	8 bolt	First row	4	4.6	HV M20 x 115	10.9	S355	4-4	50 – 8.3 / 9.1 / 10.1	11.3 / 12.7 / 14.0
		Sec. row	4					0-4	50 – 8.4 / 9.8 / 12.4	12.0 / 13.8 / 17.5
	1 bolt	-	4					4-4	35 – 9.0 / 10.6 / 13.7	13.5 / 15.2 / 18.9
M20 10.9 bolts without DTI										
DTI04	8 bolt	First row	3	1.4	HV M20 x 55	10.9	S355	3-3	14 – 4.6 / 4.8 / 5.2	7.3 / 7.6 / 8.3
		Sec. row	3					3-3	14 – 5.2 / 5.8 / 6.5	7.8 / 9.0 / 10.0
	1 bolt	-	2					2-2	14 – 5.6 / 6.4 / 7.1	8.8 / 9.6 / 10.4
DTI05	8 bolt	First row	4	2.4	HV M20 x 75	10.9	S355	4-4	14 – 4.0 / 5.1 / 6.5	6.0 / 7.7 / 9.7
		Sec. row	-					-	-	-
	1 bolt	-	4					4-4	35 – 9.4 / 10.1 / 10.8	5.5 / 6.2 / 7.1
DTI06	8 bolt	First row	4	4.4	HV M20 x 115	10.9	S355	4-4	14 – 3.6 / 4.0 / 5.0	5.3 / 6.1 / 7.6
		Sec. row	4					4-4	14 – 2.9 / 4.3 / 5.4	4.4 / 6.4 / 8.0
	1 bolt	-	3					3-3	40 – 4.7 / 5.0 / 5.5	6.6 / 7.1 / 7.7

¹⁾ clamping length ratio (Σt = clamping length and d = bolt dimension) | ²⁾ property class | ³⁾ number of bolts that achieved the preload level $F_{p,C}$

* In the first row of the 8 bolts specimens, the DTIs were placed under the nuts and in the second row, the DTIs were placed under the bolt heads and in one bolt specimens DTIs were placed under the nut.

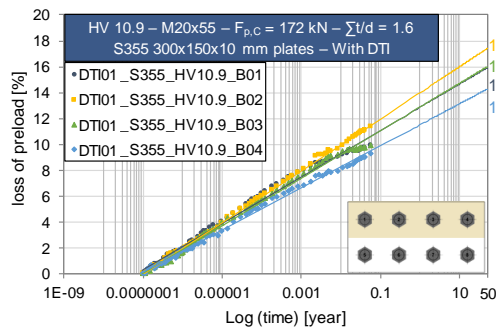
The present relaxation experiments show that the influence of positioning of the DTIs on the relaxation behaviour of the bolted connection is negligible. That means whether the DTIs were placed under the bolt head or under the nut, the same amount of loss of preload can be expected.

Table 12 Relaxation test results of M16 bolting assemblies with/without DTIs

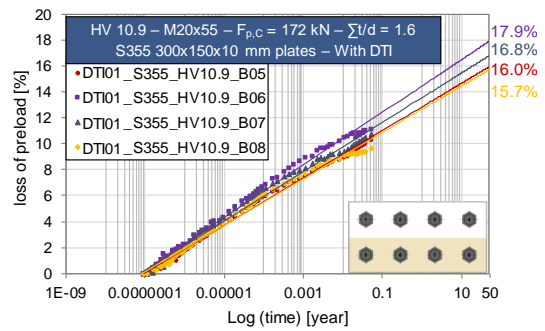
Ser. ID	Type of specimen	No. of tests	$\Sigma t/d$ ¹⁾ [-]	Bolt			Clamped plates		
				Dimension	Pc ²⁾ [-]	F _p ³⁾ [kN]	Material type	measured after days - min / mean / max [%]	after 50 years (extrapolated) min / mean / max [%]
M16 10.9 bolts with DTI									
DTI07	8 bolt	First row	4	HV M16 x 45	10.9	S355	4-4	50 –	7.6 / 9.4 / 10.5
		Sec. row	3					1.7	
	1 bolt	-	2					2-2	
DTI08	8 bolt	First row	4	HV M16 x 65	10.9	S355	4-4	50 –	6.9 / 8.4 / 10.1
		Sec. row	4					2.7	
	1 bolt	-	3					3-4	
DTI09	1bolt	-	4	HV M16 x 95			3-3	40 –	8.5 / 8.7 / 8.8
			4.7				1-4	5.9 / 6.1 / 6.3	5.8 / 7.7 / 9.0
								4.4 / 5.7 / 6.8	
M16 10.9 bolts without DTI									
DTI10	8 bolt	First row	3	HV M16 x 45	10.9	S355	4-4	14 –	7.6 / 8.6 / 9.6
		Sec. row	3					1.5	
	1bolt	-	2					3-3	
DTI11	8 bolt	First row	4	HV M16 x 65	10.9	S355	4-4	14 –	5.7 / 6.7 / 8.2
		Sec. row	4					2.5	
	1bolt	-	3					4-4	
DTI12	8 bolt	First row	4	HV M16 x 95	10.9	S355	4-4	12 –	8.2 / 8.4 / 8.8
		Sec. row	4					4.5	
	1bolt	-	2					3-3	
							2-2	40 –	7.0 / 7.0 / 7.1
								5.0 / 5.0 / 5.1	

¹⁾ clamping length ratio ($\Sigma t =$ clamping length and $d =$ bolt dimension) | ²⁾ property class | ³⁾ number of bolts that achieved the preload level $F_{p,c}$

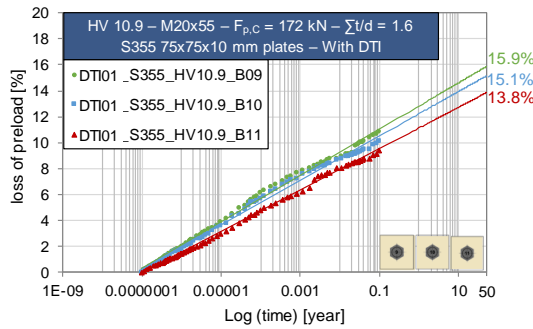
* In the first row of the 8 bolts specimens, the DTIs were placed under the nuts and in the second row, the DTIs were placed under the bolt heads and in one bolt specimens DTIs were placed under the nut.



(a) preload losses-log (time) diagrams for eight-bolts specimens - first row



(b) preload losses-log (time) diagrams for eight-bolts specimens - second row



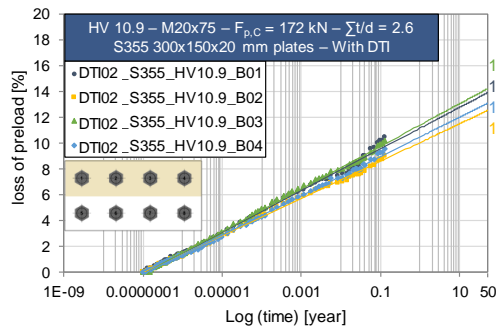
(c) preload losses-log (time) diagrams for one-bolt specimens



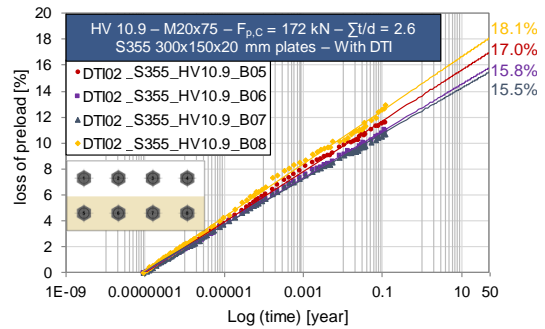
Loss of preload min / mean / max [%]	
measured after 14 days	after 50 years (extrapolated)
8.8 / 10.1 / 11.4	13.8 / 15.9 / 17.9

(d) loss of preload measured/extrapolated after 14 days/ 50 years

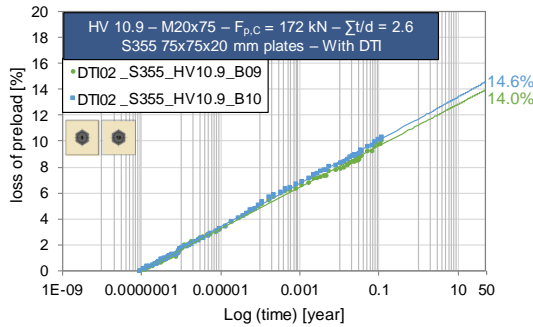
Figure 20 Preload losses for DTI01 test series



(a) preload losses-log (time) diagrams for eight-bolts specimens - first row



(b) preload losses-log (time) diagrams for eight-bolts specimens - second row



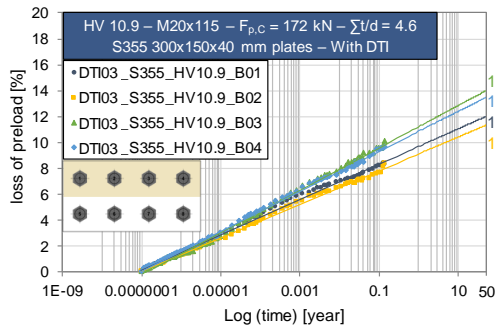
(c) preload losses-log (time) diagrams for one-bolt specimens



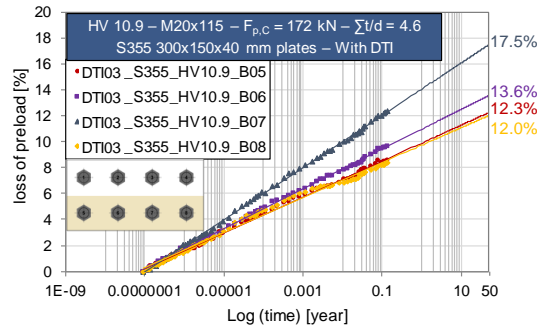
Loss of preload min / mean / max [%]	
measured after 45 days	after 50 years (extrapolated)
9.0 / 10.6 / 13.0	12.5 / 14.9 / 18.1

(d) loss of preload measured/extrapolated after 45 days/ 50 years

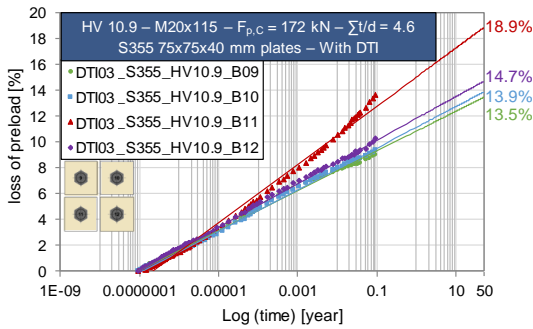
Figure 21 Preload losses for DTI02 test series



(a) preload losses-log (time) diagrams for eight-bolts specimens - first row



(b) preload losses-log (time) diagrams for eight-bolts specimens - second row



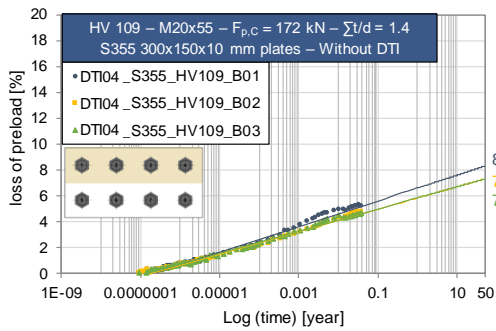
(c) preload losses-log (time) diagrams for one-bolt specimens



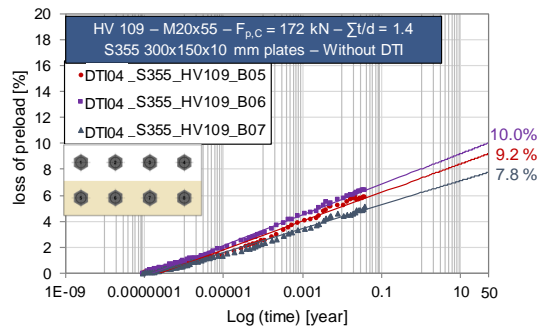
Loss of preload min / mean / max [%]	
measured after 35 days	after 50 years (extrapolated)
7.6 / 9.6 / 13.7	11.3 / 13.9 / 18.9

(d) loss of preload measured/extrapolated after 35 days/ 50 years

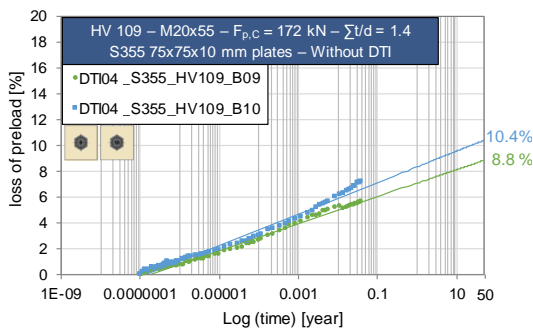
Figure 22 Preload losses for DTI03 test series



(a) preload losses-log (time) diagrams for eight-bolts specimens - first row



(b) preload losses-log (time) diagrams for eight-bolts specimens - second row



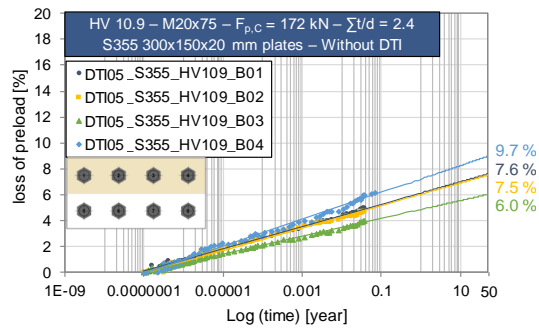
(c) preload losses-log (time) diagrams for one-bolt specimens



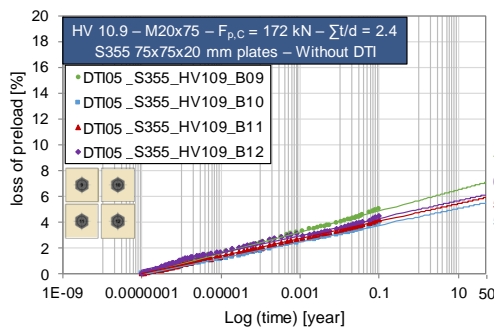
Loss of preload min /mean / max [%]	
measured after 14 days	after 50 years (extrapolated)
4.6 / 5.6 / 7.1	3.7 / 8.6 / 10.4

(d) loss of preload measured/extrapolated after 14 days/ 50 years

Figure 23 Preload losses for DTI04 test series



(a) preload losses-log (time) diagrams for eight-bolts specimens - first row



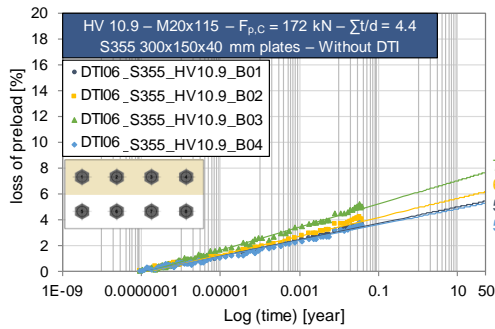
(b) preload losses-log (time) diagrams for one-bolt specimens



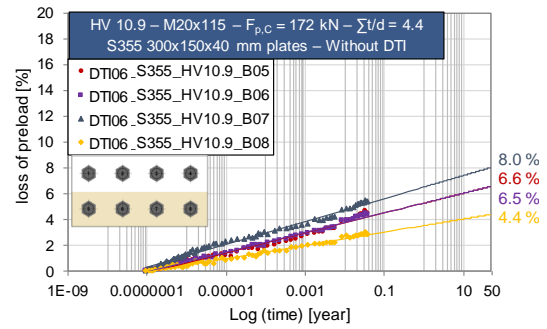
Loss of preload min / mean / max [%]	
measured after 14 days	after 50 years (extrapolated)
3.5 / 4.5 / 6.5	5.5 / 6.9 / 9.7

(c) loss of preload measured/extrapolated after 14 days/ 50 years

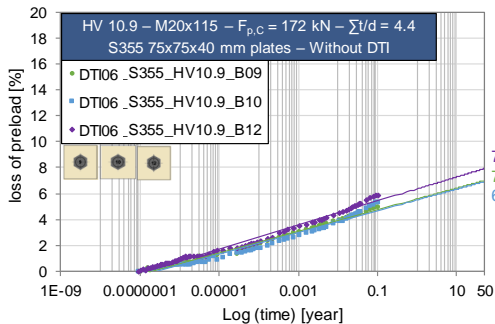
Figure 24 Preload losses for DTI05 test series



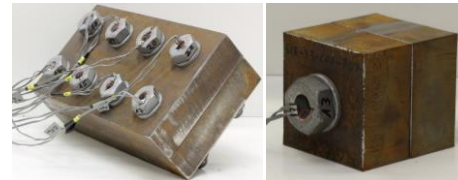
(a) preload losses-log (time) diagrams for eight-bolts specimens - first row



(b) preload losses-log (time) diagrams for eight-bolts specimens - second row



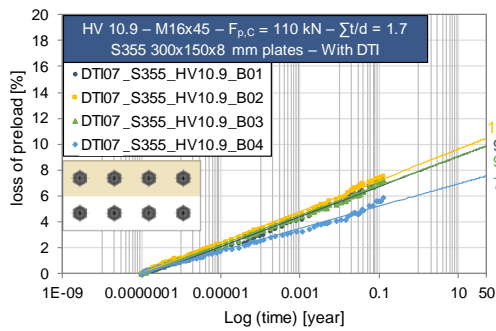
(c) preload losses-log (time) diagrams for one-bolt specimens



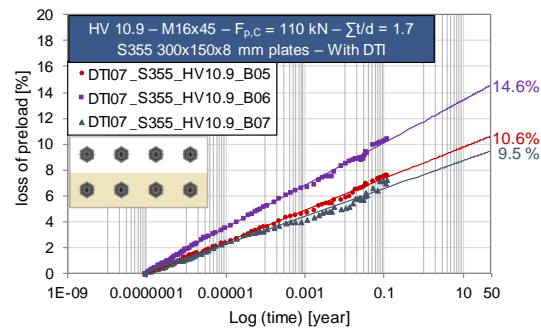
Loss of preload min / mean / max [%]	
measured after 14 days	after 50 years (extrapolated)
2.9 / 4.3 / 5.4	4.4 / 6.5 / 8.0

(d) loss of preload measured/extrapolated after 14 days/ 50 years

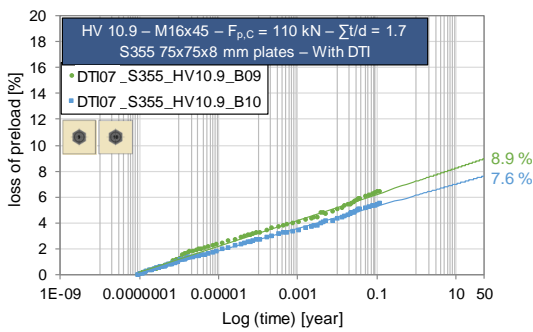
Figure 25 Preload losses for DTI06 test series



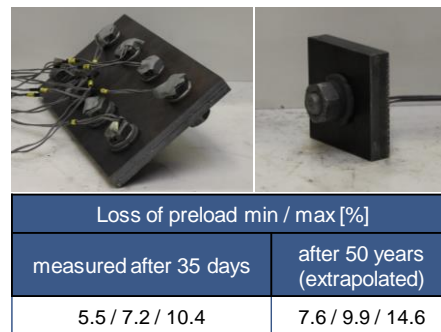
(a) preload losses-log (time) diagrams for eight-bolts specimens - first row



(b) preload losses-log (time) diagrams for eight-bolts specimens - second row

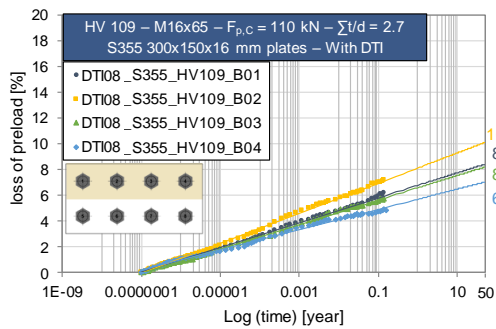


(c) preload losses-log (time) diagrams for one-bolt specimens

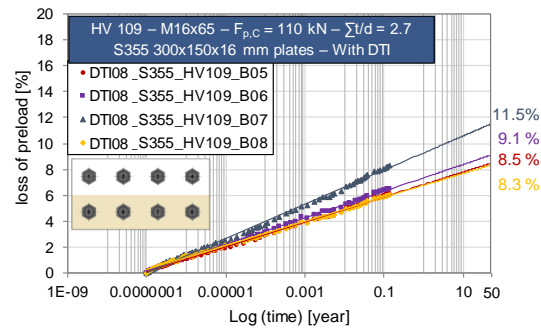


(d) loss of preload measured/extrapolated after 35 days/ 50 years

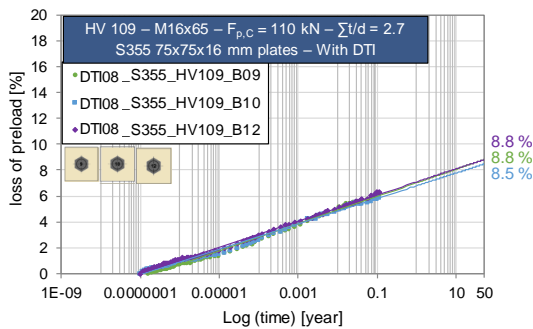
Figure 26 Preload losses for DTI07 test series



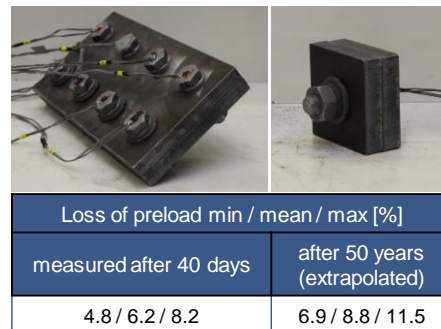
(a) preload losses-log (time) diagrams for eight-bolts specimens - first row



(b) preload losses-log (time) diagrams for eight-bolts specimens - second row

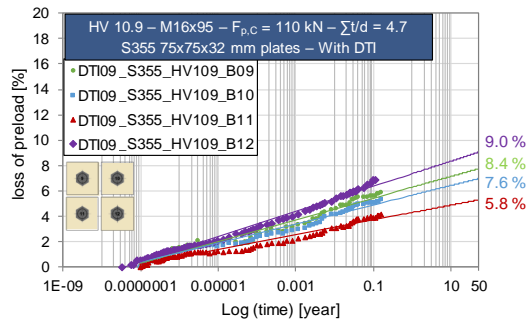


(c) preload losses-log (time) diagrams for one-bolt specimens



(d) loss of preload measured/extrapolated after 40 days/ 50 years

Figure 27 Preload losses for DTI08 test series



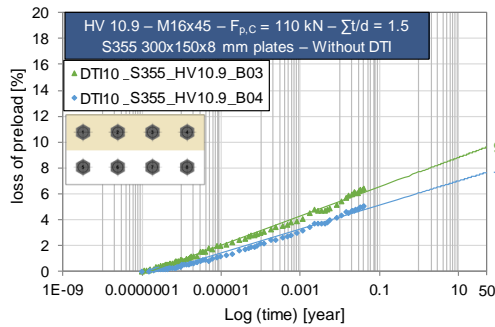
(a) preload losses-log (time) diagrams for one-bolt specimens



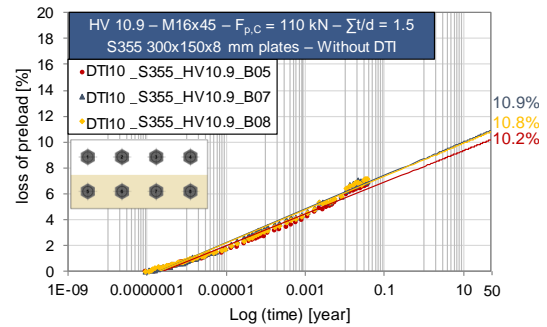
Loss of preload min / mean / max [%]	
measured after 40 days	after 50 years (extrapolated)
3.7 / 5.0 / 5.9	5.8 / 7.7 / 9.0

(b) loss of preload measured/extrapolated after 40 days/ 50 years

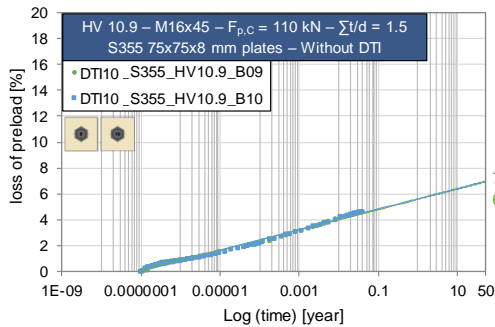
Figure 28 Preload losses for DTI09 test series



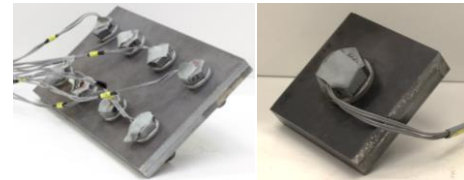
(a) preload losses-log (time) diagrams for eight-bolts specimens - first row



(b) preload losses-log (time) diagrams for eight-bolts specimens - second row



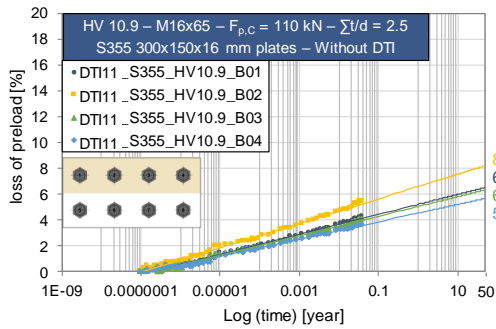
(c) preload losses-log (time) diagrams for one-bolt specimens



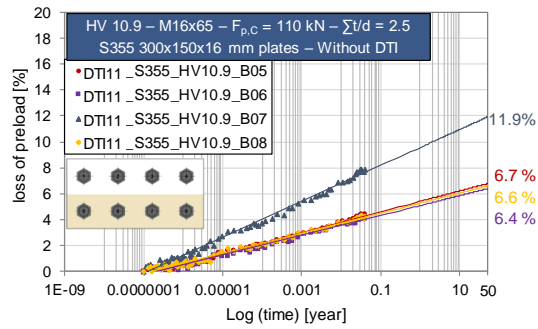
Loss of preload min / mean / max [%]	
measured after 14 days	after 50 years (extrapolated)
4.6 / 5.9 / 7.2	6.9 / 9.0 / 10.9

(d) loss of preload measured/extrapolated after 14 days/ 50 years

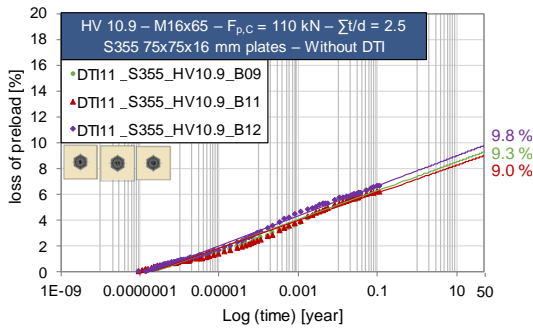
Figure 29 Preload losses for DT110 test series



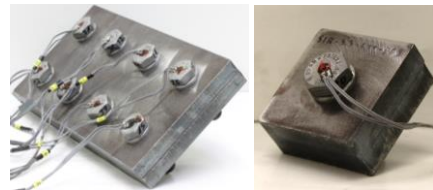
(a) preload losses-log (time) diagrams for eight-bolts specimens - first row



(b) preload losses-log (time) diagrams for eight-bolts specimens - second row



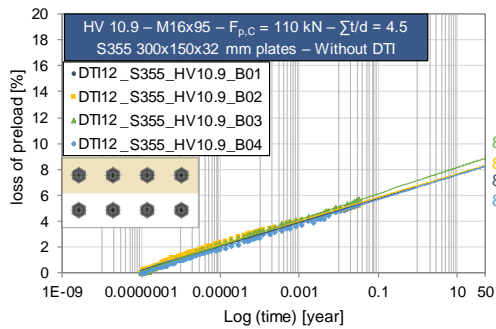
(c) preload losses-log (time) diagrams for one-bolt specimens



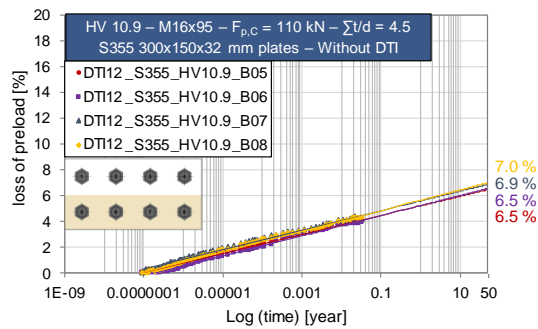
Loss of preload min / mean / max [%]	
measured after 14 days	after 50 years (extrapolated)
3.6 / 5.1 / 7.9	5.7 / 7.9 / 11.9

(d) loss of preload measured/extrapolated after 14 days/ 50 years

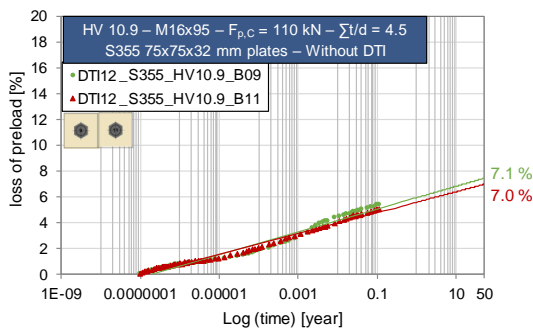
Figure 30 Preload losses for DTI11 test series



(a) preload losses-log (time) diagrams for eight-bolts specimens - first row



(b) preload losses-log (time) diagrams for eight-bolts specimens - second row



(c) preload losses-log (time) diagrams for one-bolt specimens



Loss of preload min / mean / max [%]	
measured after 12 days	after 50 years (extrapolated)
3.9 / 4.7 / 5.7	6.5 / 7.4 / 8.8

(d) loss of preload measured/extrapolated after 12 days/ 50 years

Figure 31 Preload losses for DTI12 test series

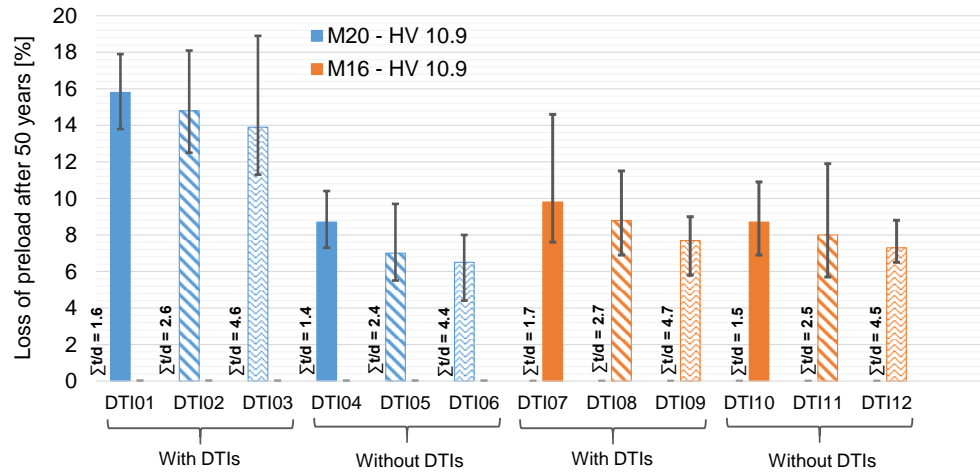


Figure 32 Extrapolated loss of preload at a service life of 50 years

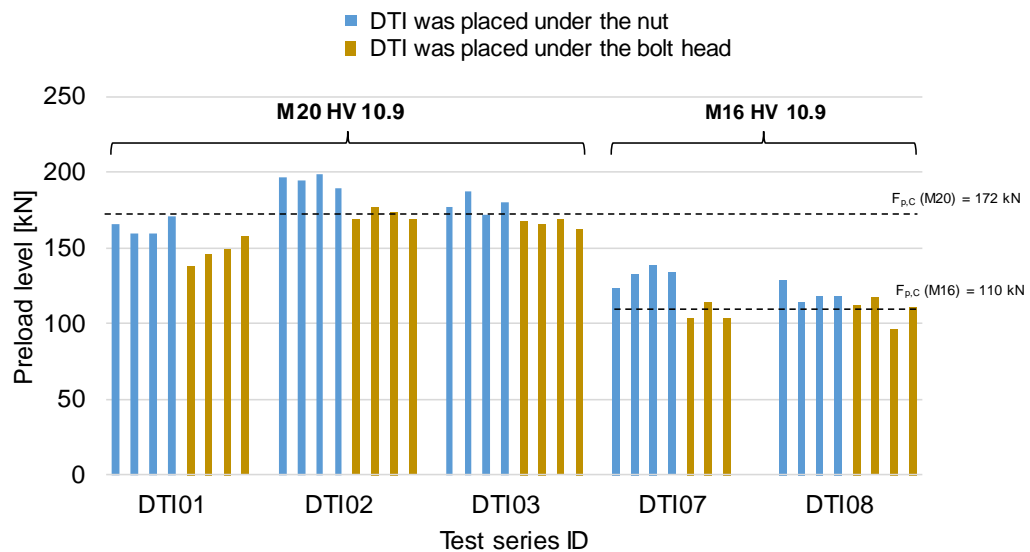
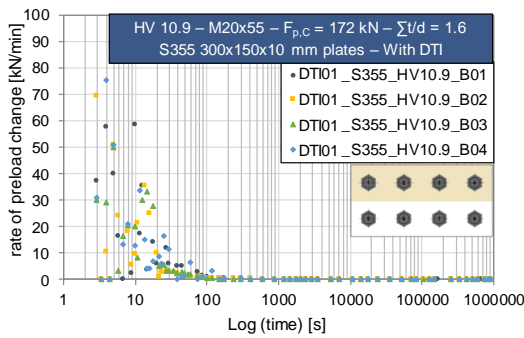


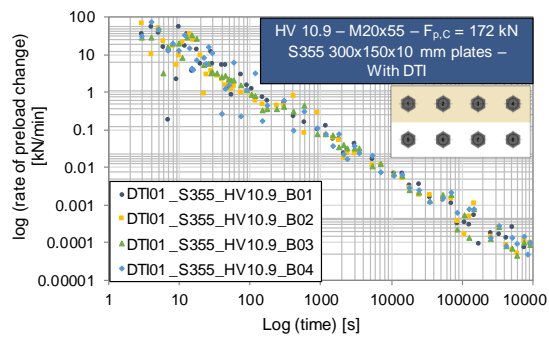
Figure 33 The achieved preload level for different DTIs bolted assemblies configurations (under the bolt head and under the nut) – results of eight-bolts-specimens

As it can be seen in Figure 33, a higher preload level was achieved by placing the DTIs under the nut compared to placing under the bolt head. Both configurations were preloaded in the same way with respect to the rotated component; the thickness of the feeler gauge was selected according to EN 14399-9. In this case, for the first row, the DTIs were placed under the nut and in the second row, they were placed under the bolt head. In both cases, the rotated component was the nut of the bolted assemblies. For this reason, the 0.25 mm and 0.4 mm feeler gauges were selected for the first and second row respectively. The results show that for M16 bolted connections with the DTIs placed under the nut and the refusals measured with 0.25 mm feeler gauge, $F_{p,C}$ was achieved in all cases. For M20, the preload level $F_{p,C}$ was achieved in most cases. However, the achieved preload level with the DTIs placed under the bolt head was always lower and in many cases the $F_{p,C}$ level was not reached.

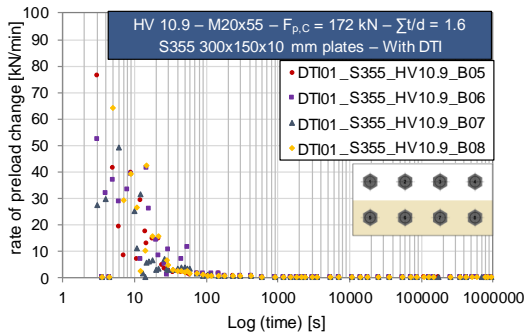
Figure 34 and Figure 35 show exemplarily the preload losses-log (time) diagrams for two different series: DTI01 and DTI04. The results show that the loss of preload starts immediately after tightening of the bolts and gradually continues as time elapses. As it can be seen from Figure 34 and Figure 35 for both test series with (DTI01) and without DTIs (DTI04) the highest rate of loss of preload is at the beginning of the test and after that the rate decreased during the passage of time. All other test results regarding the rate of loss of preload for different test series are presented in Appendix A.



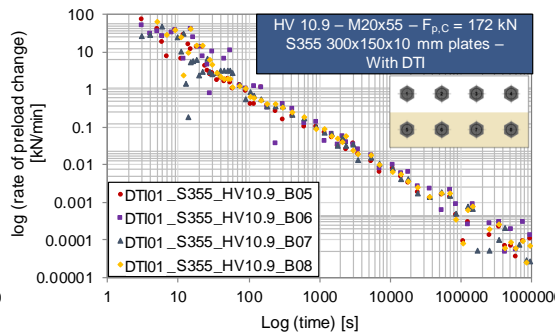
(a) log (rate of loss of preload) – time diagrams for eight-bolts specimens - first row



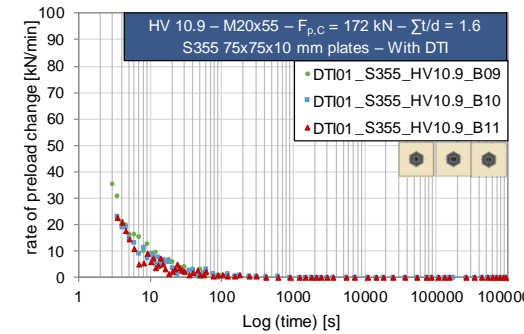
(b) log (rate of loss of preload) – log (time) diagrams for eight-bolts specimens - first row



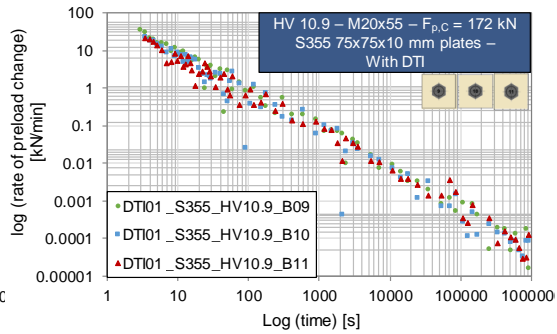
(c) log (rate of loss of preload) – time diagrams for eight-bolts specimens - second row



(d) log (rate of loss of preload) – log (time) diagrams for eight-bolts specimens - second row

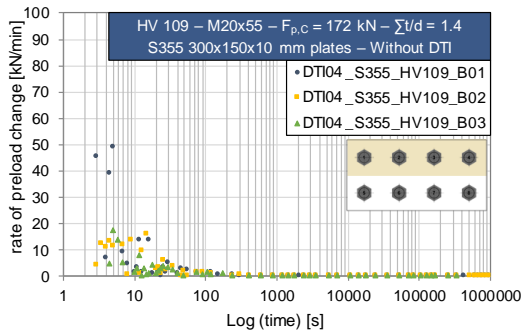


(e) log (rate of loss of preload) – time diagrams for one-bolt specimens

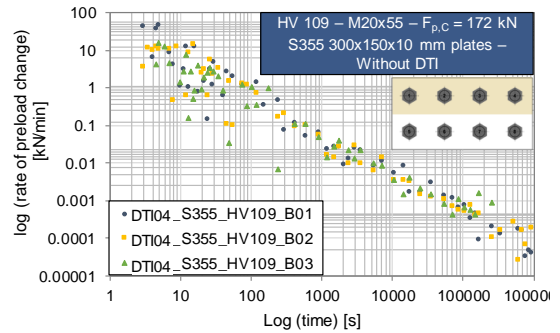


(f) log (rate of loss of preload) – log (time) diagrams for one-bolt specimens

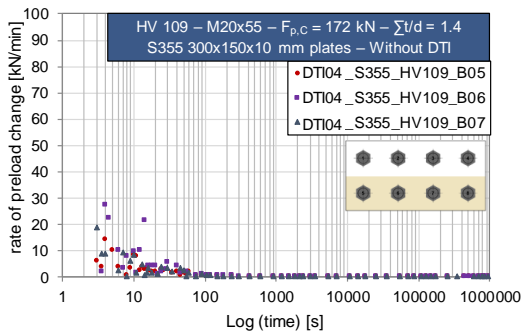
Figure 34 Rate of loss of preload for DTI01 test series (M20 bolting assemblies, goal preload level: $F_{p,c}$ 172 kN, $\sum t/d = 1.6$)



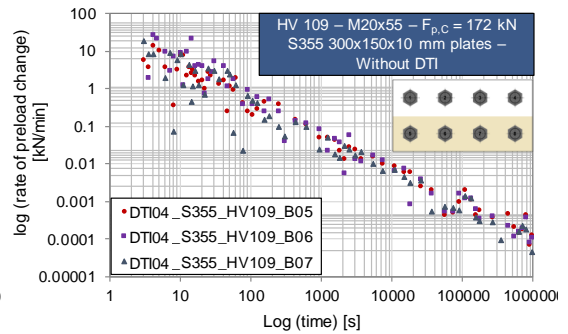
(a) log (rate of loss of preload) – time diagrams for eight-bolts specimens - first row



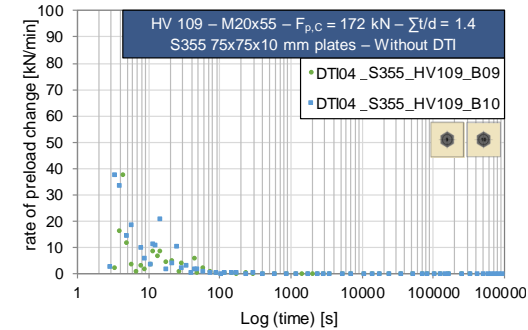
(b) log (rate of loss of preload) – log (time) diagrams for eight-bolts specimens - first row



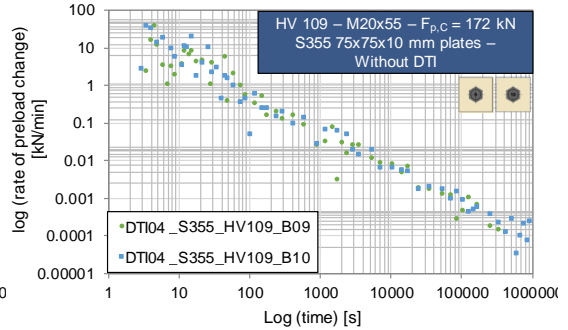
(c) log (rate of loss of preload) – time diagrams for eight-bolts specimens - second row



(d) log (rate of loss of preload) – log (time) diagrams for eight-bolts specimens - second row



(e) log (rate of loss of preload) – time diagrams for one-bolt specimens



(f) log (rate of loss of preload) – log (time) diagrams for one-bolt specimens

Figure 35 Rate of loss of preload for DTI04 test series (M20 bolting assemblies, preload level: $F_{p,C}$ 172 kN, $\Sigma t/d = 1.4$)

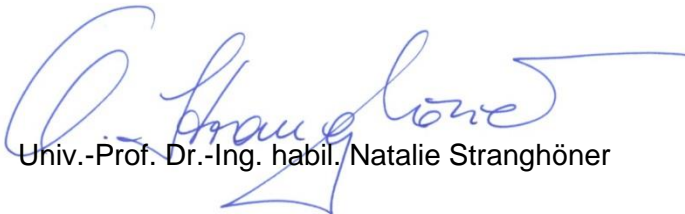
4 Conclusions

In the frame of relaxation tests under consideration of DTIs in HV bolting assemblies, carbon steel clamped plates were prepared by the Institute for Metal and Lightweight Structures of the University Duisburg-Essen. The steel plates were made of S355 according to EN 10025-2 [8].

All surfaces were tested in the "as received" surface condition. The surface roughness was measured by the Institute for Metal and Lightweight Structures according to EN ISO 4287 [9]. The measured roughness Rz of the faying surfaces varied from 6 μm to 12 μm .

The results show that the influence of the position of DTIs is negligible. It could also be shown that the loss of preload for M20 bolting assemblies with DTIs was relatively higher compared to M16 bolting assemblies. The extrapolated loss of preload at a service life of 50 years indicates that the highest loss of preload was achieved for M20 bolting assemblies with DTIs and clamping length ratio of 1.6 (about 16 %). For M16 bolting assemblies with DTIs and clamping length ratio of 1.7, this value was about 10 %. The loss of preload for M20/M16 bolting assemblies without any DTIs was about 8.5 %. This phenomenon can be ascribed to a high concentration of stress on a small area of protrusions. That results in more embedment in this area during time and consequently to higher loss of preload in these bolting assemblies.

Essen, 22.03.2018



Univ.-Prof. Dr.-Ing. habil. Natalie Stranghöner



Nariman Afzali M.Sc.

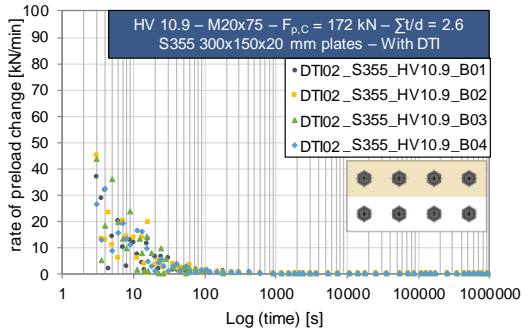


Christoph Abraham B.Sc.

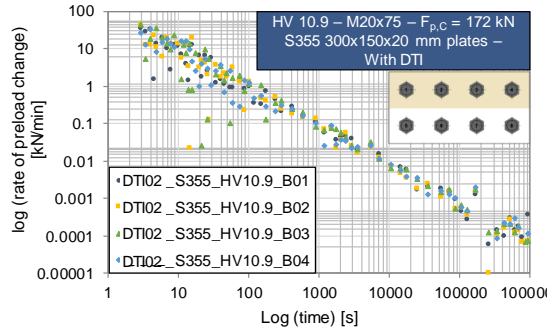
5 References

- [1] EN 1090-2:2008+A1:2011: Execution of steel structures and aluminium structures — Part 2: Technical requirements for steel structures.
- [2] EN 14399-9:2009: High-strength structural bolting assemblies for preloading – Part 9: System HR or HV – Direct tension indicators for bolt and nut assemblies.
- [3] EN 14399-4:2015: High-strength structural bolting assemblies for preloading – Part 4: System HV – Hexagon bolt and nut assemblies.
- [4] EN 14399-6:2015: High-strength structural bolting assemblies for preloading - Part 6: Plain chamfered washers.
- [5] Schiborr, M.: Zur Anwendung von direkten Kraftanzeigern in vorgespannten Verbindungen, Dissertation, Institut für Metall- und Leichtbau, Universität Duisburg-Essen, 2017.
- [6] EN 14399-2:2015: High-strength structural bolting assemblies for preloading - Part 2: Suitability for preloading
- [7] Stranghöner, N., Afzali, N.: Comparative study on the influence of bolts preloaded in the plastic range vs. bolts preloaded in the elastic range only, Deliverable report D2.2, 2018.
- [8] EN 10025-2:2004, Hot rolled products of structural steels - Part 2: Technical delivery conditions for non-alloy structural steels.
- [9] DIN EN ISO 4287:2010-07: Geometrical Product Specifications (GPS) - Surface texture: Profile method - Terms, definitions and surface texture parameters (ISO 4287:1997 + Cor 1:1998 + Cor 2:2005 + Amd 1:2009); German version EN ISO 4287:1998 + AC:2008 + A1:2009.

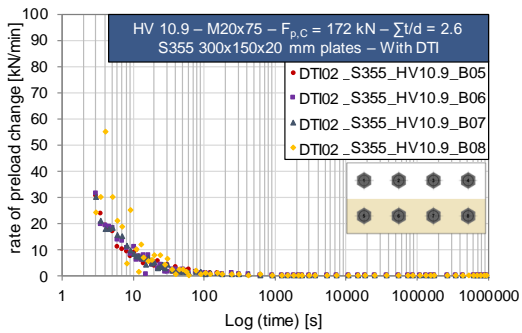
6 Annex A: Rate of loss of preload



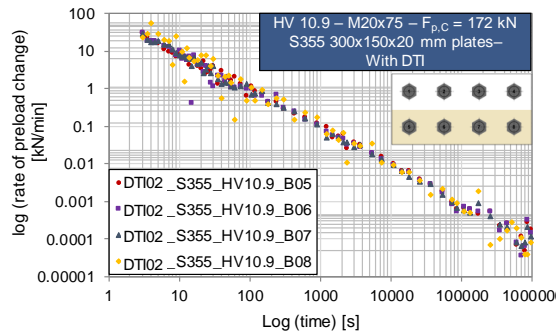
(a) log (rate of loss of preload) – time diagrams for eight-bolts specimens - first row



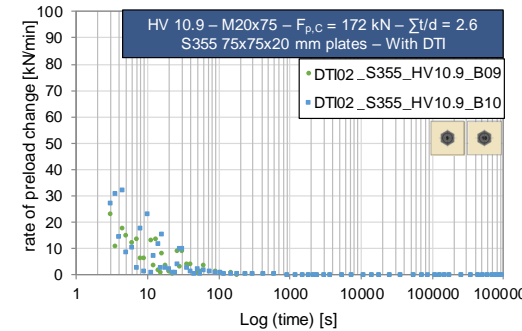
(b) log (rate of loss of preload) – log (time) diagrams for eight-bolts specimens - first row



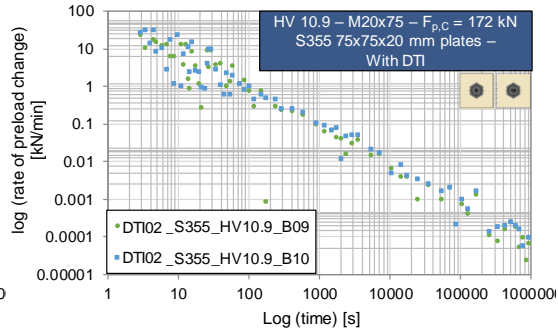
(c) log (rate of loss of preload) – time diagrams for eight-bolts specimens - second row



(d) log (rate of loss of preload) – log (time) diagrams for eight-bolts specimens - second row

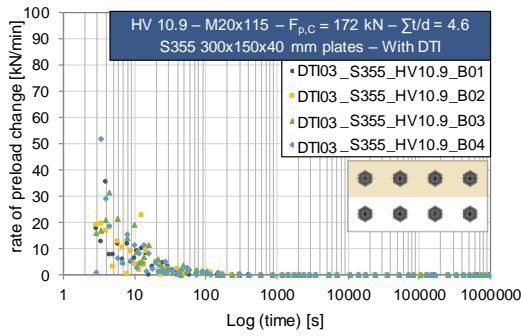


(e) log (rate of loss of preload) – time diagrams for one-bolt specimens

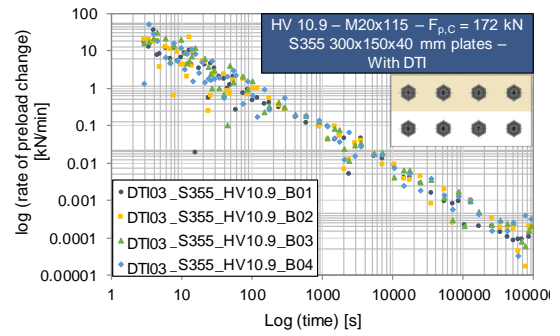


(f) log (rate of loss of preload) – log (time) diagrams for one-bolt specimens

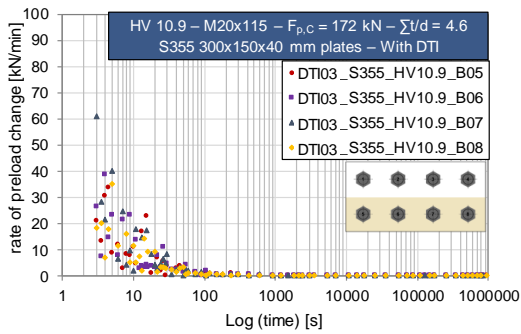
Figure 6.1 Rate of loss of preload for DTI02 test series (M20 bolting assemblies, goal preload level: $F_{p,C}$ 172 kN, $\sum t/d = 2.6$)



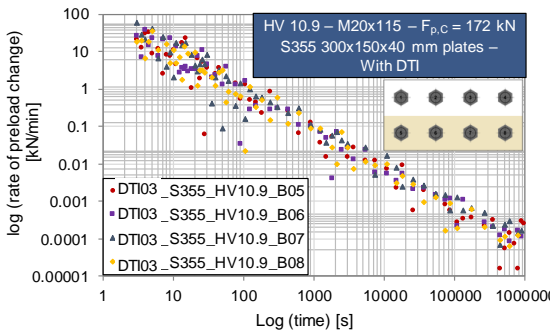
(a) log (rate of loss of preload) – time diagrams for eight-bolts specimens - first row



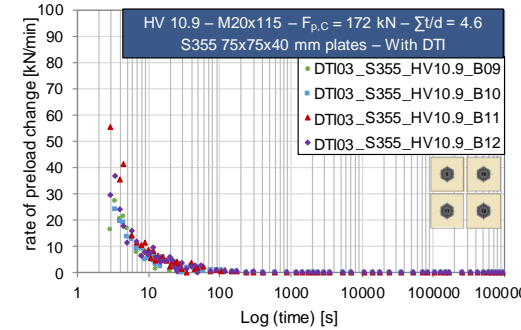
(b) log (rate of loss of preload) – log (time) diagrams for eight-bolts specimens - first row



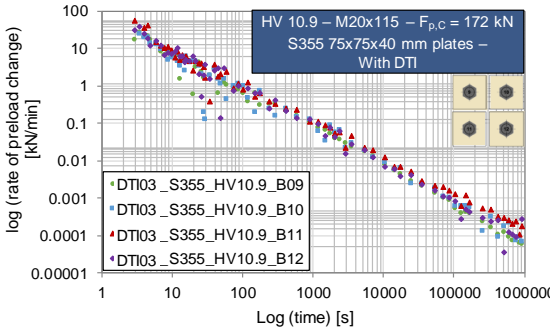
(c) log (rate of loss of preload) – time diagrams for eight-bolts specimens - second row



(d) log (rate of loss of preload) – log (time) diagrams for eight-bolts specimens - second row

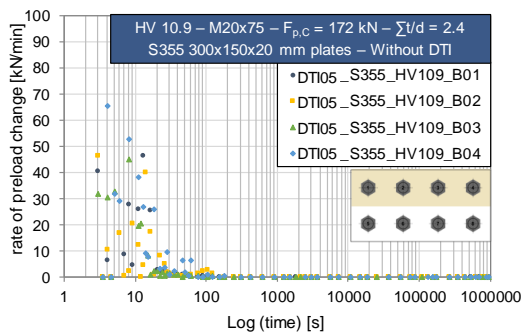


(e) log (rate of loss of preload) – time diagrams for one-bolt specimens

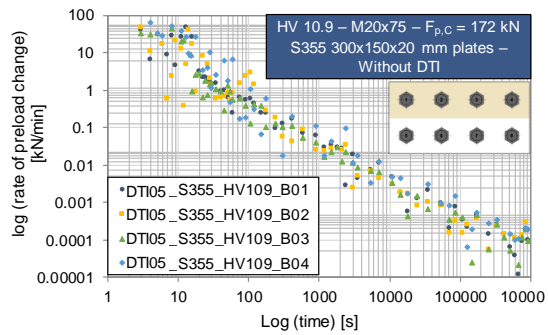


(f) log (rate of loss of preload) – log (time) diagrams for one-bolt specimens

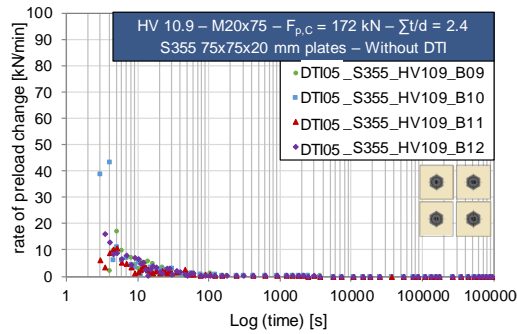
Figure 6.2 Rate of loss of preload for DTI03 test series (M20 bolting assemblies, goal preload level: $F_{p,c}$ 172 kN, $\sum t/d = 4.6$)



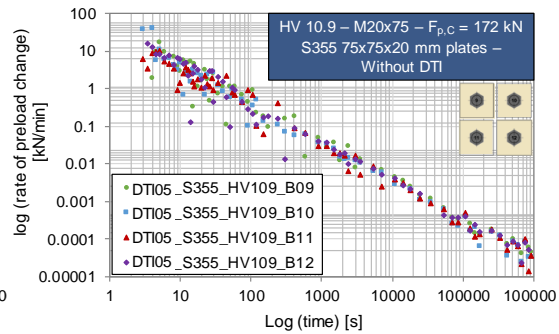
(a) log (rate of loss of preload) – time diagrams for eight-bolts specimens - first row



(b) log (rate of loss of preload) – log (time) diagrams for eight-bolts specimens - first row



(c) log (rate of loss of preload) – time diagrams for one-bolt specimens



(d) log (rate of loss of preload) – log (time) diagrams for one-bolt specimens

Figure 6.3 Rate of loss of preload for DTI05 test series (M20 bolting assemblies, preload level: $F_{p,C}$ 172 kN, $\sum t/d = 2.4$)

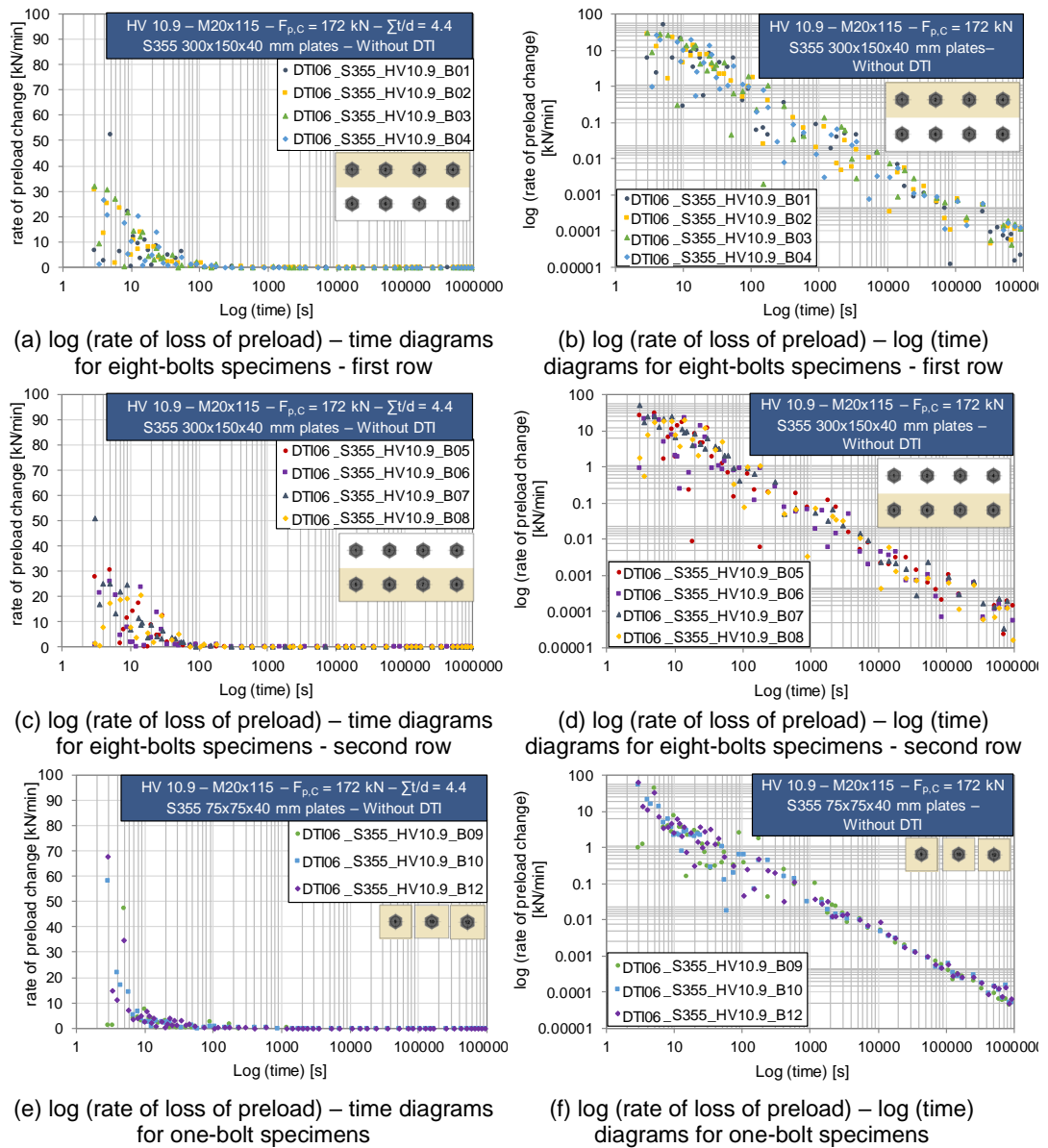
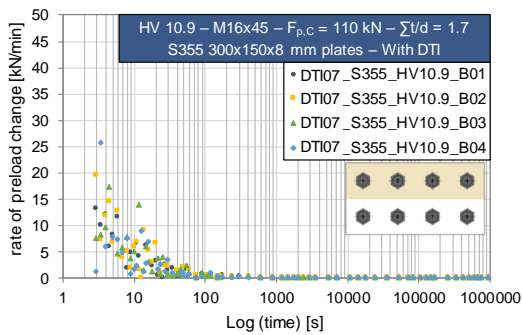
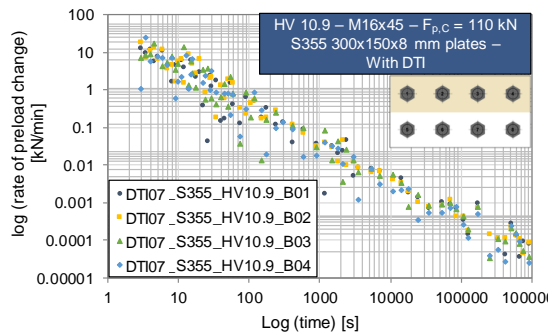


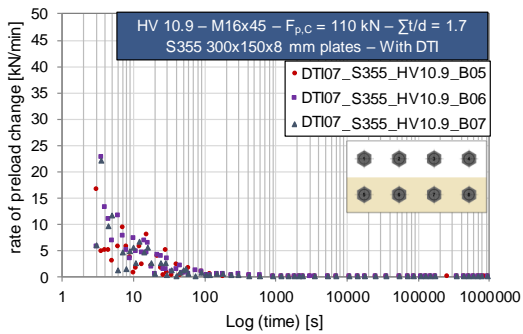
Figure 6.4 Rate of loss of preload for DTI06 test series (M20 bolting assemblies, preload level: $F_{p,C} = 172 \text{ kN}$, $\sum t/d = 4.4$)



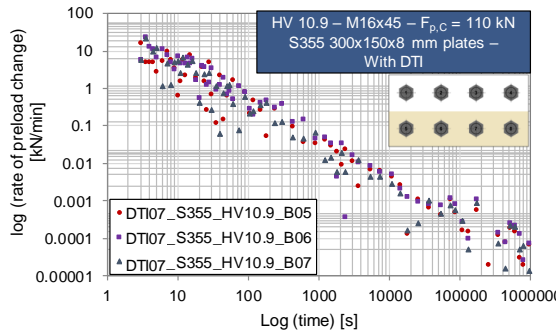
(a) log (rate of loss of preload) – time diagrams for eight-bolts specimens - first row



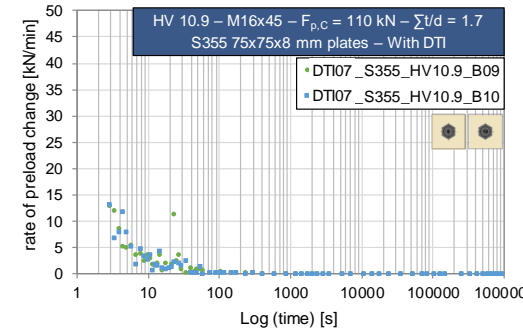
(b) log (rate of loss of preload) – log (time) diagrams for eight-bolts specimens - first row



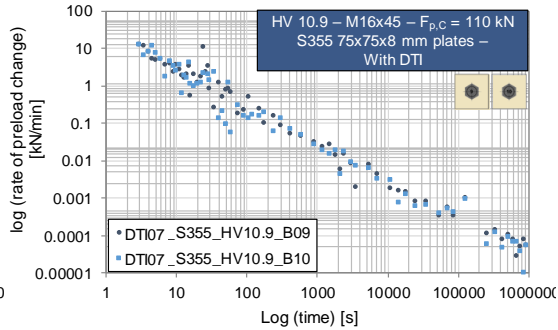
(c) log (rate of loss of preload) – time diagrams for eight-bolts specimens - second row



(d) log (rate of loss of preload) – log (time) diagrams for eight-bolts specimens - second row

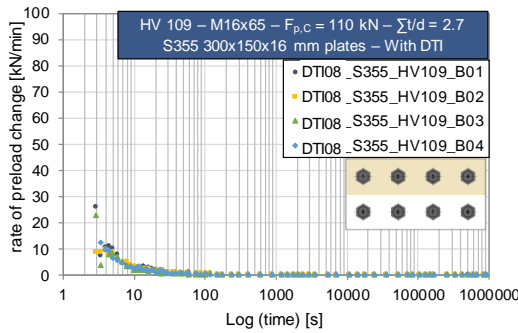


(e) log (rate of loss of preload) – time diagrams for one-bolt specimens

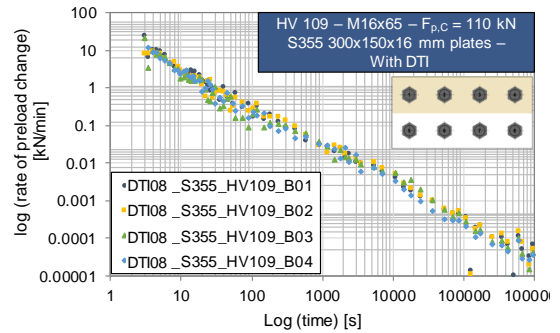


(f) log (rate of loss of preload) – log (time) diagrams for one-bolt specimens

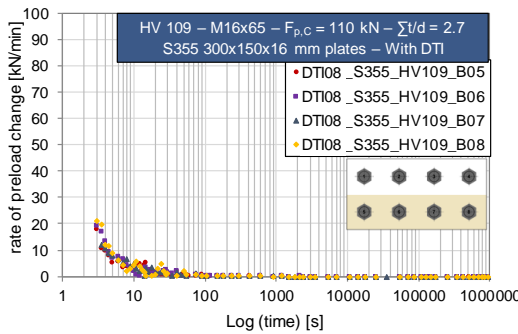
Figure 6.5 Rate of loss of preload for DTI07 test series (M16 bolting assemblies, goal preload level: $F_{p,c}$ 110 kN, $\sum t/d = 1.7$)



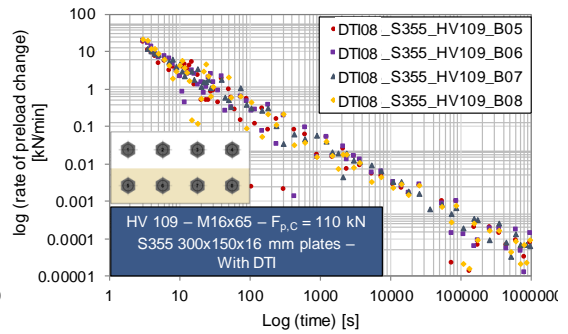
(a) log (rate of loss of preload) – time diagrams for eight-bolts specimens - first row



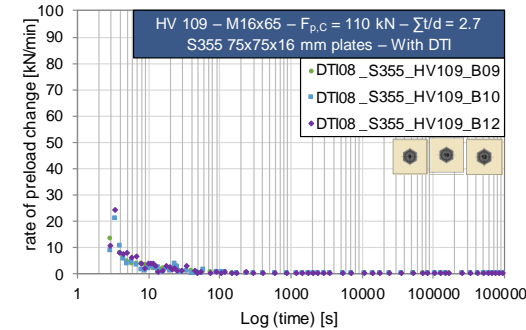
(b) log (rate of loss of preload) – log (time) diagrams for eight-bolts specimens - first row



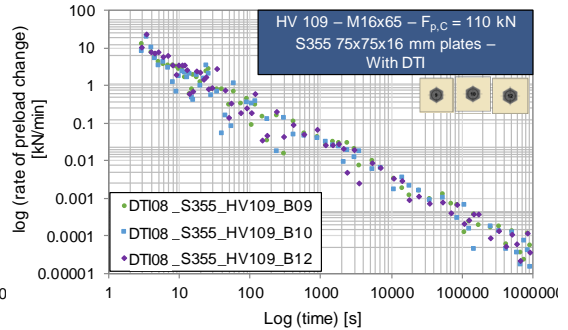
(c) log (rate of loss of preload) – time diagrams for eight-bolts specimens - second row



(d) log (rate of loss of preload) – log (time) diagrams for eight-bolts specimens - second row

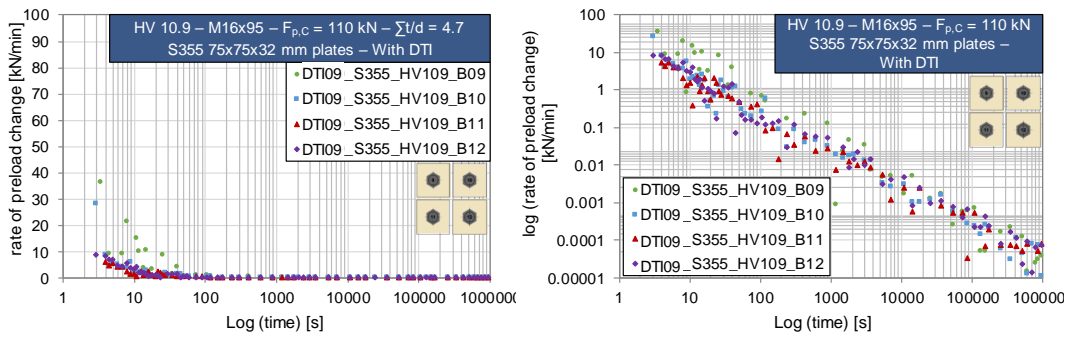


(e) log (rate of loss of preload) – time diagrams for one-bolt specimens



(f) log (rate of loss of preload) – log (time) diagrams for one-bolt specimens

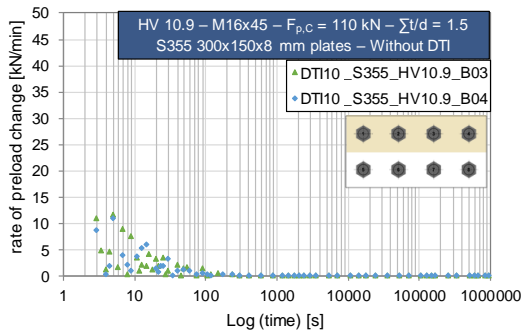
Figure 6.6 Rate of loss of preload for DTI08 test series (M16 bolting assemblies, goal preload level: $F_{p,C}$ 110 kN, $\sum t/d = 2.7$)



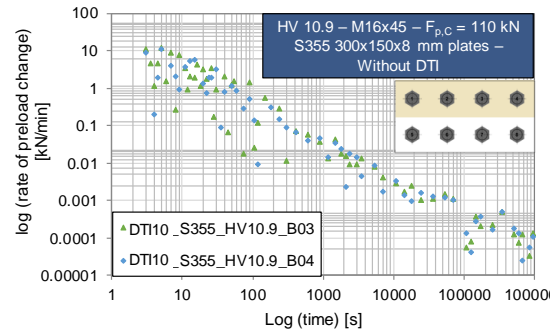
(a) log (rate of loss of preload) – time diagrams for one-bolt specimens

(b) log (rate of loss of preload) – log (time) diagrams for one-bolt specimens

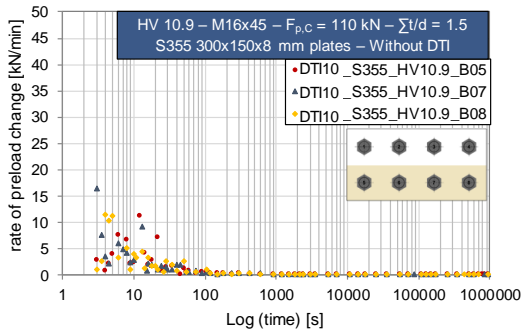
Figure 6.7 Rate of loss of preload for DTI09 test series (M16 bolting assemblies, goal preload level: $F_{p,c}$ 110 kN, $\Sigma t/d = 4.7$)



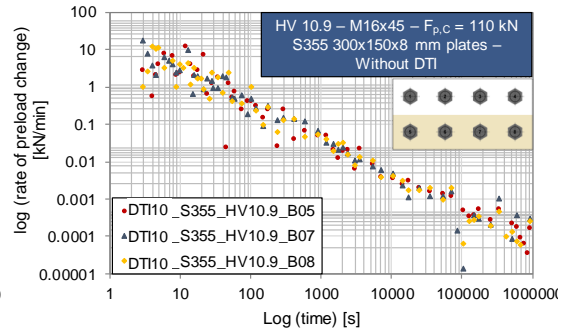
(a) log (rate of loss of preload) – time diagrams for eight-bolts specimens - first row



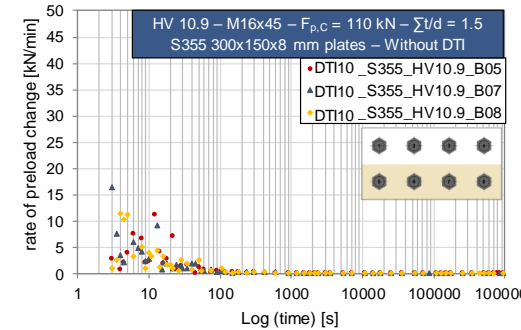
(b) log (rate of loss of preload) – log (time) diagrams for eight-bolts specimens - first row



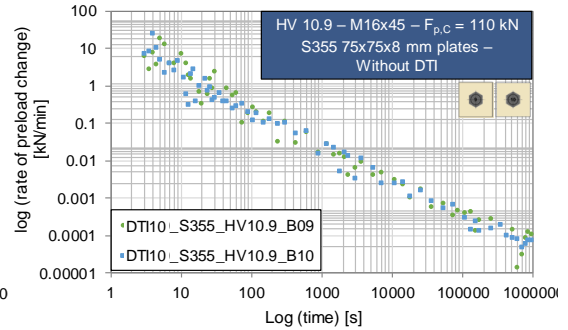
(c) log (rate of loss of preload) – time diagrams for eight-bolts specimens - second row



(d) log (rate of loss of preload) – log (time) diagrams for eight-bolts specimens - second row

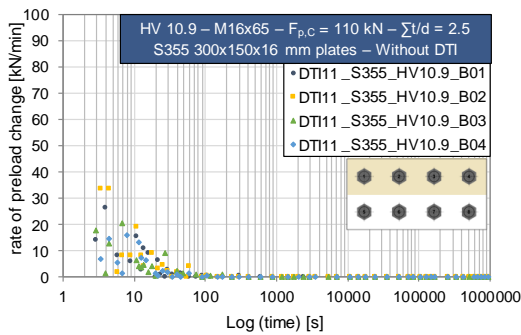


(e) log (rate of loss of preload) – time diagrams for one-bolt specimens

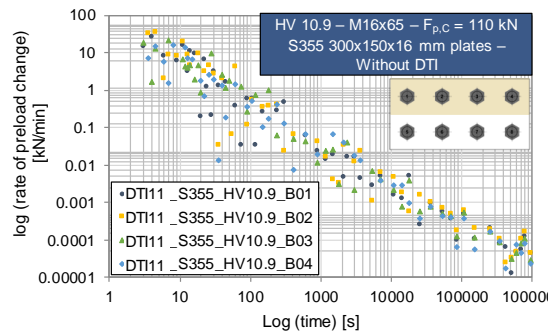


(f) log (rate of loss of preload) – log (time) diagrams for one-bolt specimens

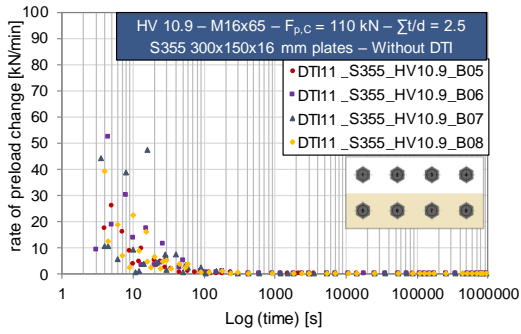
Figure 6.8 Rate of loss of preload for DTI10 test series (M16 bolting assemblies, preload level: $F_{p,C} = 110 \text{ kN}$, $\sum t/d = 1.5$)



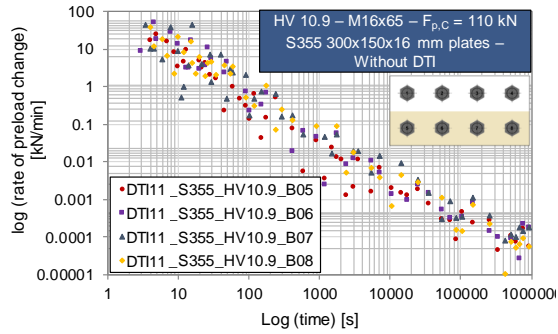
(a) log (rate of loss of preload) – time diagrams for eight-bolts specimens - first row



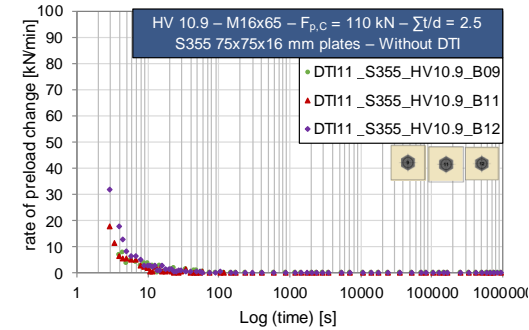
(b) log (rate of loss of preload) – log (time) diagrams for eight-bolts specimens - first row



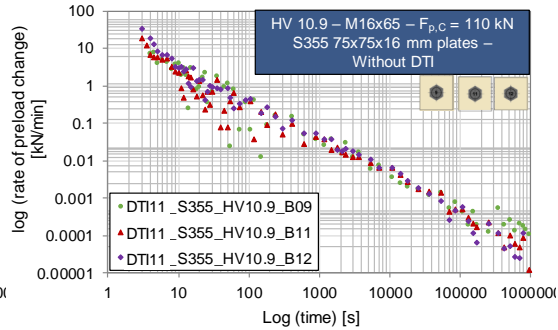
(c) log (rate of loss of preload) – time diagrams for eight-bolts specimens - second row



(d) log (rate of loss of preload) – log (time) diagrams for eight-bolts specimens - second row

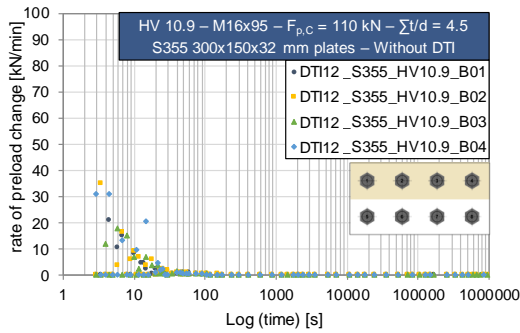


(e) log (rate of loss of preload) – time diagrams for one-bolt specimens

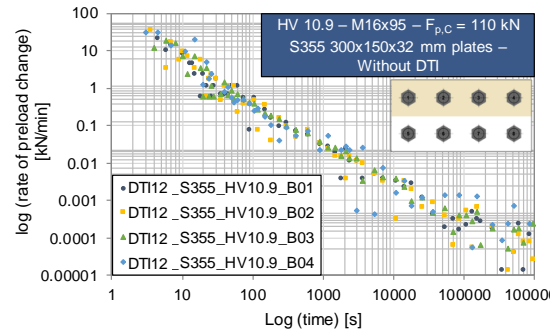


(f) log (rate of loss of preload) – log (time) diagrams for one-bolt specimens

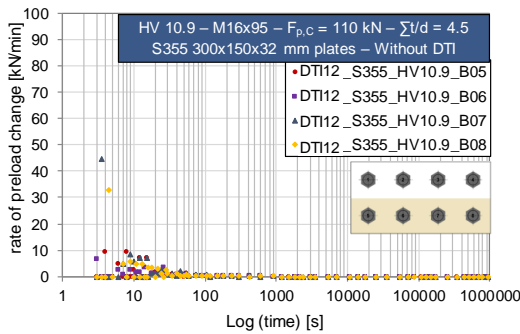
Figure 6.9 Rate of loss of preload for DTI11 test series (M16 bolting assemblies, preload level: $F_{p,C}$ 110 kN, $\Sigma t/d = 2.5$)



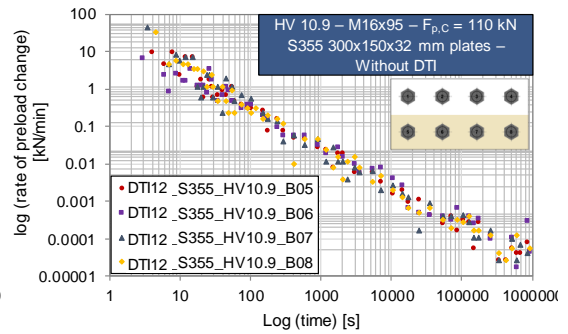
(a) log (rate of loss of preload) – time diagrams for eight-bolts specimens - first row



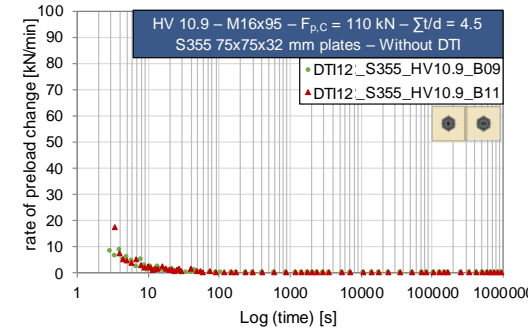
(b) log (rate of loss of preload) – log (time) diagrams for eight-bolts specimens - first row



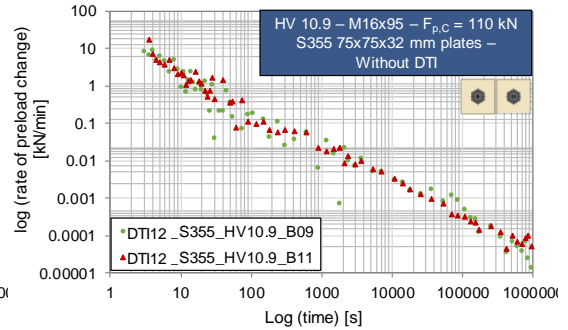
(c) log (rate of loss of preload) – time diagrams for eight-bolts specimens - second row



(d) log (rate of loss of preload) – log (time) diagrams for eight-bolts specimens - second row



(e) log (rate of loss of preload) – time diagrams for one-bolt specimens



(f) log (rate of loss of preload) – log (time) diagrams for one-bolt specimens

Figure 6.10 Rate of loss of preload for DTI12 test series (M16 bolting assemblies, preload level: $F_{p,C}$ 110 kN, $\sum t/d = 4.5$)